The Abdus Salam
International Centre for Theoretical Physics

United Nations
Educational, Scientific
and Cultural Organization

International Atomic
Energy Agency

SMR 1673/11

AUTUMN COLLEGE ON PLASMA PHYSICS

5 - 30 September 2005

Drift Instabilities in Magnetically Confined Plasmas: A Brief Overview

A. Hirose

Plasma Physics Laboratory, University of Saskatchewan, Canada

Strada Costiera 11, 34014 Trieste, Italy - Tel. +39 040 2240 111; Fax +39 040 224 163 - sci_info@ictp.it, www.ictp.it

Autumn College on Plasma Physics

International Centre for Theoretical Physics, Trieste, Italy

September 2005

Drift Instabilities in Magnetically Confined Plasmas: A Brief Overview

A. Hirose

Plasma Physics Laboratory, University of Saskatchewan

116 Science Place, Saskatoon, Saskatchewan S7N 5E2, Canada

1 Introduction

The particle and energy confinement times in magnetically confined plasmas are anomalously short compared with those expected from the classical collisional transport theories. The anomaly is attributed to suprathermal fluctuations widely observed in the density, temperature, potential, and magnetic field. The existence of turbulence in magnetically confined plasmas is well expected since the pressure gradient, which is maintained by the magnetic Lorentz force through the force balance $\nabla p = \mathbf{J} \times \mathbf{B}$, can act as a source of free energy that can be released through plasma instabilities.

Theoretical studies of the drift mode in magnetically confined plasmas have a long history, and date back to the original work in the early 1960s. (For a review of the earlier work, see [1 Mikhailovskii].) The discovery of the drift instability was based on a local analysis in a shearless slab geometry in which $k_{||}$, the wavenumber along the ambient magnetic field, is well defined and constant. A methodology was later developed for nonlocal analysis [2 Krall, 3 Pearlstein] in sheared slab geometry and a criterion for suppressing the instability by magnetic shear was found. More rigorous analysis in sheared slab geometry showed that the drift mode should be stable no matter how weak was the magnetic shear [4 Ross-Mahajan, 5 Tsang et al.] However, in the toroidicity induced drift mode [6, 7], shear stabilization is unable to overcome toroidicity induced destabilization. (The slab mode considered in [4, 5] remains stable in toroidal geometry.) Furthermore, in toroidal geometry, the stabilizing ion Landau damping can effectively be suppressed by the ion magnetic drift for modes propagating in the direction of the electron diamagnetic drift, such as the toroidal drift mode. The toroidal ion temperature gradient (ITG) mode [8 Jarmen] is driven by the resonance at the ion magnetic drift frequency and propagates in the direction of the ion diamagnetic drift.

In tokamaks, a large number of drift-type modes driven by density and/or temperature gradients are expected to be unstable. Drift modes driven by trapped electrons and the ion temperature gradient have been the subjects of extensive theoretical investigations because of their relatively large growth rates and long wavelengths. The most rapidly growing mode is the electron temperature gradient (ETG) mode [9 Lee, Dong, et al.] which has a growth rate of the order of the electron transit frequency $\gamma \simeq v_{Te}/qR$ where $v_{Te} = \sqrt{2T_e/m_e}$ is the electron thermal speed and qR is the connection length. In tokamaks and other magnetic confinement devices, various drift type instabilities driven by pressure gradient can occur over a wide range of cross-field wavelengths. There are numerous dimensionless parameters that characterize a tokamak discharge, including s (magnetic shear), q (safety factor), β_e ($= 2\mu_0 p_e/B^2$, electron beta factor), β_i ($= 2\mu_0 p_i/B^2$, ion beta factor), $\alpha = q^2 R\beta/L_p$ (the ballooning parameter with L_p the pressure gradient scale length), $\varepsilon = r/R$ (inverse aspect ratio), A (isotopic number), and so on. In drift stability analyses, dependence of the growth rates on those parameters is of a primary interest, for it may open a path for stabilization.

The drift modes are predominantly electrostatic. In general, a finite β ($\beta = 2\mu_0 p/B^2$) has stabilizing effects on the ITG mode [10 Weiland/Hirose] but destabilizing effects on the trapped electron driven drift mode. Electromagnetic (finite β) effects on the ITG mode can be analyzed in terms of the same mode equation as used for the kinetic ballooning mode which caused some confusion in the past.

In this lecture, the pressure gradient driven drift modes in magnetically confined plasmas (tokamaks, in particular) are reviewed together with several methodologies frequently used in analyzing the instabilities. Mixing length estimate for ion and electron thermal diffusivities will be outlined. The ultimate objective of studying drift modes is in gaining a better understanding of the roles played by them in anomalous transport and, possibly, in finding means to suppress them.

2 Drift Mode Basics

The plasma equilibrium condition $\nabla p = \mathbf{J} \times \mathbf{B}$ yields the following current perpendicular to the magnetic field,

$$\mathbf{J}_* = \frac{\mathbf{B} \times \nabla p}{B^2}. \tag{1}$$

This current flows in such a way as to reduce the magnetic field and is thus called the diamagnetic current. It consists of electron and ion components,

$$\mathbf{J}_* = \frac{\mathbf{B} \times \nabla p}{B^2} = \frac{\mathbf{B}}{B^2} \times \nabla(n_0 T_e + n_0 T_i). \tag{2}$$

The electron diamagnetic current has two parts, one due to the density gradient and another due to the temperature gradient,

$$\mathbf{J}_{*e} = \frac{\mathbf{B}}{B^2} \times \nabla(n_0 T_e) = \frac{\mathbf{B}}{B^2} \times (T_e \nabla n_0 + n_0 \nabla T_e). \tag{3}$$

The electron diamagnetic drift velocity is normally defined by

$$\mathbf{V}_{*e} = \frac{T_e}{eB^2 n_0} \boldsymbol{\nabla} n_0 \times \mathbf{B}, \tag{4}$$

where $e > 0$ is the electronic charge. (A neutral plasma with singly charged ions is assumed throughout.) The diamagnetic current is not a result of guiding center drift. Rather, it is due to an effective mass flow created by the density imbalance in neighboring Larmor circles and the diamagnetic current is in fact a part of the magnetization current due to nonuniformity in the magnetic dipole moment density. For example, the electron magnetization current is by definition

$$\mathbf{J}_{Me} = -\nabla \times \left(\frac{p_e}{B^2}\mathbf{B}\right) = \frac{\mathbf{B} \times \nabla p_e}{B^2} + 2\frac{\nabla B \times \mathbf{B}}{B^3}p_e - \frac{p_e}{B^2}\nabla \times \mathbf{B}, \tag{5}$$

In the RHS, the first term is the diamagnetic current and the second term is due to the nonuniformity in the magnetic field. In a low β plasma, it is exactly cancelled by the guiding center drifts due to the magnetic gradient and curvature,

$$\mathbf{J}_{\nabla B} = n_0 \left\langle \frac{\mathbf{B} \times \nabla B}{B^3}\frac{1}{2}m_e v_\perp^2 + \frac{\mathbf{B} \times (\mathbf{B} \cdot \nabla \mathbf{B})}{B^4}m_e v_\parallel^2 \right\rangle \simeq 2\frac{\mathbf{B} \times \nabla B}{B^3}p_e, \tag{6}$$

provided the magnetic gradient and curvature are equal $B\nabla B \simeq \mathbf{B} \cdot \nabla \mathbf{B}$ which holds in low β plasmas. Here $\langle \cdots \rangle$ indicates averaging over the velocity with Maxwellian weighting,

$$\left\langle m_e v_\perp^2 \right\rangle = 2T_e, \quad \left\langle m_e v_\parallel^2 \right\rangle = T_e. \tag{7}$$

(That the nonuniformity in a magnetic field does not produce a net current was elucidated by Tonks [11]. A static magnetic field does not do any work on charged particles and thus will not modify particle distribution functions.) In low β plasmas, the third term, $-p_e\nabla \times \mathbf{B}/B^2$, is negligible.

In toroidal devices such as tokamaks and stellarators, the magnetic field is nonuniform, and the divergence of the diamagnetic current does not vanish,

$$\nabla \cdot \mathbf{J}_\perp = \nabla \cdot \mathbf{J}_* = -\frac{2}{B^3}\nabla B \cdot (\mathbf{B} \times \nabla p). \tag{8}$$

Then, the charge neutrality condition $\nabla \cdot \mathbf{J} = \nabla \cdot \mathbf{J}_\perp + \nabla \cdot \mathbf{J}_\parallel = 0$ can be satisfied only if a current parallel to the magnetic field $\mathbf{J}_\parallel$ exists. This parallel current is called the rotational transform current (also called Pfirsch-Schlüter current) and plays important roles in plasma confinement. (In tokamaks, the rotational transform current flows in addition to the current externally driven (*e.g.*, Ohmic current) to create the poloidal magnetic field B_θ. $J_\parallel$ modifies the poloidal magnetic field and causes a shift of the magnetic axis as will be shown.)

Although the diamagnetic drift velocity $\mathbf{V}_{*e}$ is not a guiding center drift, a density perturbation created in a magnetically confined plasma propagates approximately at this velocity provided electrons obey the Boltzmann distribution (thermal equilibrium)

$$N_e = n_0 \exp\left(-\frac{-e\phi}{T_e}\right) = n_0 \exp\left(\frac{e\phi}{T_e}\right), \tag{9}$$

where $-e\phi$ is the potential energy of electrons. This occurs when the wave frequency ω is sufficiently low compared with the electron transit frequency $\omega \ll k_\parallel v_{Te}$, where $k_\parallel$ is the field gradient along the magnetic field and v_{Te} is the electron thermal speed. In this case, electron temperature equilibration along the magnetic field takes place rapidly, and the electron temperature is not perturbed. If $e\phi \ll T_e$, the electron density perturbation is

$$n_e = n_0 \exp\left(\frac{e\phi}{T_e}\right) - n_0 \simeq \frac{e\phi}{T_e} n_0. \tag{10}$$

To see the propagation of the drift mode in the electron diamagnetic direction, let us consider the linearized lowest order continuity equation of the ions,

$$\frac{\partial n_i}{\partial t} + \mathbf{v}_E \cdot \nabla n_0 + n_0 \nabla \cdot \mathbf{v}_{pi} = 0, \tag{11}$$

where

$$\mathbf{v}_E = \frac{\mathbf{E} \times \mathbf{B}}{B^2} = \frac{\mathbf{B} \times \nabla\phi}{B^2}, \tag{12}$$

is the $E \times B$ drift velocity with the scalar potential ϕ and $\mathbf{v}_{pi}$ is the ion polarization drift velocity,

$$\mathbf{v}_{pi} = \frac{e}{m_i \omega_{ci}^2} \frac{d}{dt} \mathbf{E}_\perp = -\frac{e}{m_i \omega_{ci}^2} \frac{d}{dt} (\nabla_\perp \phi). \tag{13}$$

(In Eq. (11), magnetic curvature (toroidicity) and ion velocity perturbation along the magnetic field are ignored.) These drift velocities can be found from the equation of motion for the ion in the low frequency limit $\omega \ll \omega_{ci}$,

$$m_i \frac{d\mathbf{v}_i}{dt} = e\left(\mathbf{E}_\perp e^{-i\omega t} + \mathbf{v}_i \times \mathbf{B}\right). \tag{14}$$

In the lowest order, the time derivative can be ignored, and the $E \times B$ drift emerges,

$$\mathbf{v}_E = \frac{\mathbf{E}_\perp \times \mathbf{B}}{\mathbf{B}^2} e^{-i\omega t}. \tag{15}$$

To find the velocity in the order ω/ω_{ci}, let the magnetic field be in the z direction and the time varying electric field in the x direction, Then,

$$\left(\frac{d^2}{dt^2} + \omega_{ci}^2\right) v_x = \frac{e}{m_i} \frac{d}{dt} E_x e^{-i\omega t}. \tag{16}$$

and Eq. (13) follows. Assuming all perturbed quantities are proportional to $e^{i(\mathbf{k}\cdot\mathbf{x}-\omega t)}$, we find from Eq. (11),

$$n_i = \frac{\omega_{*e} - \omega\left(k_\perp \rho_s\right)^2}{\omega}\frac{e\phi}{T_e}n_0, \tag{17}$$

where

$$\omega_{*e} = \mathbf{k}\cdot\mathbf{V}_{*e} = \frac{T_e k_\theta}{eBL_n}, \tag{18}$$

is the electron diamagnetic drift frequency, L_n is the radial density gradient scale length, k_θ is the wavenumber in the azimuthal (θ) direction, and

$$\rho_s = \frac{\sqrt{T_e/m_i}}{\omega_{ci}}, \tag{19}$$

is the ion Larmor radius with the electron temperature. Note that $k_\perp^2 = k_\theta^2 + k_r^2 = k_\theta^2 - \partial^2/\partial r^2$.

Equating n_i to n_e (charge neutrality condition), we find a dispersion relation,

$$\omega = \frac{\omega_{*e}}{1+\left(k_\perp \rho_s\right)^2} = \frac{V_{*e}k_\theta}{1+(k_\theta^2+k_r^2)\rho_s^2},\ \ T_e \gg T_i. \tag{20}$$

The wave propagates in the direction of V_{*e} (the electron diamagnetic drift velocity). A finite ion temperature does not alter this basic picture. When $T_e \gg T_i$, the above dispersion relation is valid at arbitrary $k_\perp \rho_s$. In an isothermal plasma with $T_i \simeq T_e$ as tokamaks, a correction due to a finite ion Larmor radius enters in the form

$$\omega \simeq \frac{1-\left(k_\perp \rho_i\right)^2}{1+\left(k_\perp \rho_s\right)^2}\omega_{*e},\ \ \left(k_\perp \rho_i\right)^2 \ll 1. \tag{21}$$

where $\rho_i = \sqrt{T_i/m_i}/\omega_{ci}$ is the ion Larmor radius. When $T_i \simeq T_e$, $\rho_s \simeq \rho_i$, and the dispersion relation is valid only in the long wavelength regime $\left(k_\perp \rho_s\right)^2 \ll 1$.Then, the drift wave frequency remains close to ω_{*e}.

The progressive propagation of the drift wave in the direction $\nabla n_0 \times \mathbf{B}$ is schematically illustrated in Fig. 1. The equilibrium density gradient is in the $-x$ direction with $dn_0/dx < 0$, the magnetic field in the z direction, and the wave propagation in the y direction. A potential perturbation of $\phi_0 \sin(ky)$ and electric field of $E_y = -k\phi_0 \cos(ky)$ are shown. The density perturbation is proportional to ϕ. The $E \times B$ drift in the positive electric field region is in $+x$ direction, and the plasma moves from the higher density region to the lower density region. Therefore, the perturbation progressively shifts in the y direction which is in the electron diamagnetic drift V_{*e}. The situation is similar to the ion acoustic wave described by $\omega = kc_s$ in which electrons provide elasticity through the pressure $p_e = n_0 T_e$ and ions provide inertia. The main difference is that in the case of ion acoustic wave, energy equipartition holds between the ion kinetic energy and potential energy, while in the case of long wavelength drift mode, the ion kinetic energy is subdominant. The ion kinetic energy density in the ion acoustic wave is $n_0 m_i v_i^2/2$. Substitution of the velocity perturbation from

$$m_i \frac{\partial v_i}{\partial t} = eE = -e\frac{\partial \phi}{\partial x}, \tag{22}$$

we readily find that the ion kinetic energy density is equal to the electron potential energy density,

$$\frac{1}{2} n_0 m_i v_i^2 = \frac{1}{2} n_0 T_e \left(\frac{n_e}{n_0}\right)^2, \tag{23}$$

where $n_e = (e\phi/T_e)\, n_0$ is the electron density perturbation as in the case of the drift wave. In the drift wave, however, such energy equipartition does not hold and energy density is dominated by the potential energy, since the ion kinetic energy density is

$$\frac{1}{2} n_0 m_i v_i^2 = \frac{1}{2} n_0 m_i \left(\frac{E_\perp}{B}\right)^2 = \frac{1}{2}\left(\frac{\omega_{pi}}{\omega_{ci}}\right)^2 \varepsilon_0 E_\perp^2 = \frac{1}{2}\left(\frac{\omega_{pi}}{\omega_{ci}}\right)^2 \varepsilon_0 \left(k\phi_0\right)^2 \cos^2\left(kx\right), \tag{24}$$

while the potential energy density is

$$\frac{1}{2} n_0 T_e \left(\frac{n_e}{n_0}\right)^2 = \frac{1}{2}\left(\frac{e\phi_0}{T_e}\right)^2 n_0 T_e \sin^2\left(kx\right). \tag{25}$$

The peak value of the kinetic energy density is smaller than that of the potential energy density by a factor $(k_\perp \rho_s)^2$ $(\ll 1)$. Here $\omega_{pi} = \sqrt{n_0 e^2/\varepsilon_0 m_i}$ is the ion plasma frequency and $\varepsilon_\perp \simeq (\omega_{pi}/\omega_{ci})^2\, \varepsilon_0$ is the cross field permittivity. In the drift mode, the region of small finite ion Larmor radius parameter $(k_\perp \rho_s)^2 \simeq (k_\perp \rho_i)^2 \ll 1$ $(T_i \simeq T_e)$ is of main concern, for long wavelength fluctuations are considered to be more dangerous for plasma confinement. (A rough estimate of anomalous thermal diffusivity is $\chi \simeq \gamma/k_\perp^2$ where γ is the growth rate and $k_\perp = 2\pi/\lambda_\perp$ is the wavenumber.)

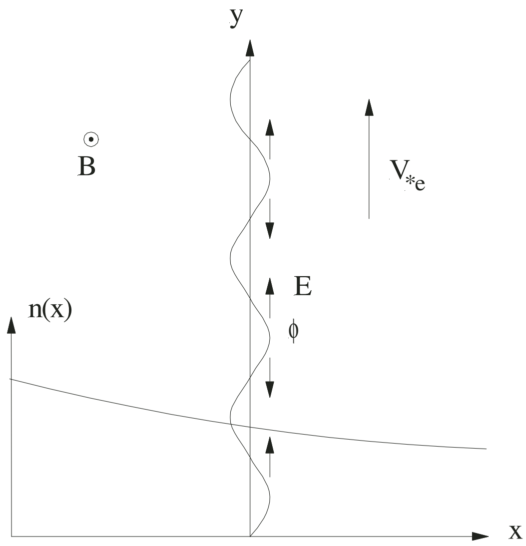

Fig. 1. Sinusoidal potential-density ($\phi \propto n$) and electric field (E) perturbations propagate upward because in the region $E > 0$ (upward), $E \times B$ drift is from higher to lower density region.

In the course of this derivation, the assumption of adiabatic electron response immediately yielded the electron density perturbation in terms of the potential ϕ. Let us see if the density perturbation is consistent with the electron continuity equation. (It should be.) Substitution of the electron adiabatic response

$$n_e = \frac{e\phi}{T_e} n_0, \tag{26}$$

into the electron continuity equation,

$$\frac{\partial n_e}{\partial t} + \mathbf{v}_E \cdot \nabla n_0 + n_0 \nabla \cdot \mathbf{v}_{e\parallel} = 0, \tag{27}$$

yields the electron flow along magnetic field,

$$v_{e\parallel} = \frac{\omega - \omega_{*e}}{k_\parallel} \frac{e\phi}{T_e}, \tag{28}$$

or the electron current perturbation along the magnetic field,

$$J_{e\parallel} = \frac{n_0 e^2}{k_\parallel T_e} (\omega_{*e} - \omega)\, \phi. \tag{29}$$

This is consistent with the electron parallel velocity expected from the perturbed electron distribution function [1],

$$f_e = \frac{e\phi}{T_e} f_{Me} - \frac{\omega - \omega_{*e}}{\omega - k_\parallel v_\parallel} \frac{e\phi}{T_e} f_{Me}, \tag{30}$$

where f_{Me} is the Maxwellian electron distribution function. In the limit $\omega \ll k_\parallel v_{Te}$, we indeed find

$$v_{e\parallel} = \langle v_\parallel \rangle = \frac{\omega - \omega_{*e}}{k_\parallel} \frac{e\phi}{T_e}. \tag{31}$$

The parallel current $J_{e\parallel}$ is thus redundant in electrostatic cases. (It is not needed.) If a vector potential parallel to the magnetic field is perturbed, the electron current density in the same limit $\omega \ll k_\parallel v_{Te}$ becomes

$$J_{e\parallel} = \frac{n_0 e^2}{k_\parallel T_e} \left((\omega_{*e} - \omega) \phi + \frac{(\omega - \omega_{*e})(\omega - \omega_{De}) + \eta_e \omega_{*e} \omega_{De}}{k_\parallel} A_\parallel \right), \tag{32}$$

and plays a more prominent role. Here ω_{De} is the electron magnetic drift frequency due to nonuniformity in the magnetic field and $\eta_e = d \ln T_e / d \ln n_0$ is the electron temperature gradient parameter.

The kinetic electron density perturbation can be found by integrating f_e in Eq. (30) over the velocity,

$$n_e = \left(1 + \frac{\omega - \omega_{*e}}{k_\parallel v_{Te}} Z(\zeta) \right) \frac{e\phi}{T_e} n_0, \tag{33}$$

where $Z(\zeta) = Z\left(\omega / k_\parallel v_{Te}\right)$ is the plasma dispersion function [12 Fried and Conte] defined by

$$Z(\zeta) = \frac{1}{\sqrt{\pi}} \int_{-\infty}^{\infty} \frac{e^{-x^2}}{x - \zeta} dx. \tag{34}$$

If $\zeta \ll 1$, then $Z(\zeta) \simeq i\sqrt{\pi}$, and we find

$$n_e \simeq \left(1 + i\sqrt{\pi} \frac{\omega - \omega_{*e}}{k_\parallel v_{Te}} \right) \frac{e\phi}{T_e} n_0. \tag{35}$$

Then the dispersion relation becomes

$$\frac{\omega_{*e} - \omega (k_\perp \rho_s)^2}{\omega} = 1 + i\sqrt{\pi} \frac{\omega - \omega_{*e}}{k_\parallel v_{Te}}, \tag{36}$$

which yields an unstable solution

$$\omega \simeq \frac{\omega_{*e}}{1 + (k_\perp \rho_s)^2} + i \frac{\omega_r^2}{k_\parallel v_{Te}} (k_\perp \rho_s)^2. \tag{37}$$

Note that the necessary condition for the drift instability is $\omega < \omega_{*e}$, that is, the cross field phase velocity along the direction of V_{*e} be smaller than the electron diamagnetic drift velocity V_{*e}. This may be regarded as a Cerenkov condition and the instability is a result of inverse Landau damping by electrons.

3 Quasi-linear Fluxes

The quasilinear theory has originally been developed for velocity space instabilities such as the beam-plasma instabilities. It is the lowest order nonlinear theory in the sense that mode coupling is ignored entirely. As such, quasilinear theory is unable to accurately predict the energy spectrum of fluctuations. In the case of velocity space instabilities, modification in the original linearly unstable velocity distribution leads to saturation. However, in drift type modes which are driven by spatial nonuniformities, the density and temperature profiles are maintained by external sources through fuelling and heating and saturation must be invoked by other mechanism.

Let us consider low frequency electrostatic fluctuations which cause particles to undergo $E \times B$ drift,

$$\mathbf{v}_k = c\frac{\mathbf{B} \times \nabla\phi_k}{B^2}. \tag{38}$$

The particle flux induced by the fluctuations can be calculated from the statistical average of the following quadratic quantity,

$$\Gamma = \text{ Re } \langle n_k \mathbf{v}_k \rangle , \tag{39}$$

where n is the density fluctuation and $\langle \cdots \rangle$ indicates statistical ensemble average. In quasilinear theory, the density fluctuation is approximated by the linear response which in the lowest order can be found from the continuity equation,

$$\frac{\partial n_k}{\partial t} + \mathbf{v}_k \cdot \nabla n_0 = 0.$$

This yields

$$n_k = \frac{\omega_{*k}}{\omega}\frac{e\phi_k}{T}n_0, \tag{40}$$

where $\omega = \omega_k + i\gamma_k$ is the complex frequency. Substituting this into Eq. (39), we obtain the following expression for the radial flux,

$$\Gamma_r = \sum_k \frac{\gamma_k \omega_{*k}}{\omega_k^2 + \gamma_k^2}\frac{Tk_\theta}{eB}\left(\frac{e\phi_k}{T}\right)^2 n_0. \tag{41}$$

This is an anomalous particle flux due to exponentially growing mode, $\phi_k(t) = \phi_k(0)e^{\gamma_k t}$. Of course, in experiments, fluctuations are observed to be stationary on average and the linear growth rate appearing in Eq. (41) must be modified somehow to be physically meaningful.

Stationary fluctuations observed in experiments do not mean they are pure sinusoidal functions of time. They grow and damp intermittently and only on time average they are stationary. Pure sinusoidal fluctuations are characterized by an infinitely long correlation time. The correlation time is a measure of average life time of each Fourier component and can be deduced from the auto correlation function,

$$\Phi_k(s) = \langle \phi_k(t)\phi_k(t+s)\rangle_t \,, \tag{42}$$

where $\langle \cdots \rangle_t$ indicates time averaging. The auto-correlation function often exhibits exponential decay,

$$\Phi_k(s) = \Phi_k(0)\cos(\omega_k s)\exp\left(-\frac{s}{\tau_k}\right). \tag{43}$$

τ_k is defined as the correlation time. As a rough approximation, τ_k may be estimated from the linear growth rate,

$$\tau_k \simeq \frac{1}{\gamma_k}, \tag{44}$$

and the flux in Eq. (41) may be used in steady state turbulence.

The particle diffusivity D defined by

$$\Gamma_r = -D\frac{dn_0}{dr}, \tag{45}$$

takes the following form

$$D = \sum_k \frac{\gamma_k \omega_{*k}}{\omega_k^2+\gamma_k^2}\frac{Tk_\theta L_n}{eB}\left(\frac{e\phi_k}{T}\right)^2. \tag{46}$$

The fluctuation level ϕ_k in Eq. (46 is yet to be determined. As mentioned earlier, the quasilinear theory is unable to predict the saturation level. In drift type modes, two dimensional $E\times B$ motion leads to formation of vortices in which particles are trapped. Once trapped, the instability becomes saturated because wave-particle interaction for wave growth is deactivated. The condition for vortex formation is

$$v_{E\times B} \gtrsim \frac{\omega}{k_\perp} \simeq \frac{T}{eBL_n} \text{ (diamagnetic velocity)}. \tag{47}$$

This yields

$$\frac{e\phi_k}{T} \simeq \frac{1}{k_\perp L_n}, \tag{48}$$

and the diffusivity becomes

$$D = \sum_k \frac{\gamma_k \omega_{*k}}{\omega_k^2 + \gamma_k^2} \frac{T}{eB} \frac{1}{k_\perp L_n} \simeq \frac{T}{eB} \sum_k \frac{1}{k_\perp L_n}, \tag{49}$$

provided $\omega_k \simeq \gamma_k \simeq \omega_{*k}$. Since the growth rate of drift modes peaks at a specific finite Larmor radius parameter $k_\perp \rho$, the diffusivity may be written as

$$D = \text{const}\ \frac{T}{eB} \frac{\rho}{L_n}. \tag{50}$$

(For example, the growth rate of the toroidal ITG mode peaks at $k_\perp \rho_s \simeq 0.3$.) This form of diffusivity is known as the gyro-Bohm diffusivity (the Bohm diffusivity $D_B = T/eB$ corrected for the gyro-radius ρ). If, on the other hand, the cross-filed scale length $1/k_\perp$ does not scale with the Larmor radius, but with plasma size, $1/k_\perp \simeq a$, the resultant diffusivity is Bohm-like,

$$D = \ \text{const}\ \frac{T}{eB}. \tag{51}$$

Another estimate for saturation is based on

$$k_r v_k \simeq \gamma_k, \tag{52}$$

where k_r is the radial wavenumber. Physically, this condition implies that saturation occurs when the nonlinear Doppler shift, $k_\perp v_k$, becomes comparable with the growth rate. The saturated amplitude in this case is given by

$$\frac{e\phi_k}{T} \simeq \frac{\gamma_k}{k_r^2} \frac{eB}{T}, \tag{53}$$

and the diffusivity by

$$D = \sum_k \frac{\gamma_k^3}{\omega_r^2 + \gamma_k^2} \frac{1}{k_r^2}. \tag{54}$$

In strong turbulence limit, $\gamma_k > \omega_k$, we recover the familiar form,

$$D = \sum_k \frac{\gamma_k}{k_r^2}. \tag{55}$$

4 Effects of Finite Ion Temperature

The basic mechanism of drift instability is wave amplification through the Cerenkov mechanism, and for an instability to occur, the wave phase velocity in the direction of the electron diamagnetic drift must be smaller than the electron diamagnetic velocity $\omega/k_\theta < V_{*e}$. The simple mode

$\omega = \omega_{*e}/\left[1+(k_\perp\rho_s)^2\right] < \omega_{*e}$ found in the preceding section is potentially unstable. A finite ion temperature and toroidicity further reduce the frequency. Let us first find what effective electric field is seen by the guiding center of an ion undergoing cyclotron motion with a Larmor radius $\rho = v_\perp/\omega_{ci}$. If the electric field is uniform, the ion experiences the same field everywhere. However, if the field has a sinusoidal spatial dependence in the direction perpendicular to the magnetic field,

$$E_\perp(\mathbf{r}) = E_0 e^{i\mathbf{k}_\perp\cdot\mathbf{r}}, \tag{56}$$

an average over the Larmor orbit must be taken. Expansion of $E_\perp(\mathbf{r})$ about the guiding center denoted by $\mathbf{r}_g$ yields

$$E_\perp\left[\mathbf{r}_g+\boldsymbol{\rho}(t)\right] = E_\perp(\mathbf{r}_g) + \boldsymbol{\rho}\cdot\frac{\partial E_\perp}{\partial \mathbf{r}} + \frac{1}{2}\left(\boldsymbol{\rho}\cdot\frac{\partial}{\partial \mathbf{r}}\right)^2 E_\perp + \cdots, \tag{57}$$

where $\boldsymbol{\rho}(t)$ is the instantaneous ion location relative to the guiding center. Averaging along the ion orbit, we find an effective electric field seen by a gyrating ion,

$$\langle E_\perp\rangle = \left(1-\frac{1}{4}(k_\perp\rho)^2+\frac{1}{64}(k_\perp\rho)^4-\cdots\right)E_0 e^{i\mathbf{k}_\perp\cdot\mathbf{r}} = J_0(k_\perp\rho)\,E_0 e^{i\mathbf{k}_\perp\cdot\mathbf{r}}, \tag{58}$$

where J_0 is the Bessel function of order 0 defined by

$$J_0(x) = \sum_{n=0}^{\infty}\frac{(-1)^n}{(n!)^2}\left(\frac{x}{2}\right)^{2n} = 1-\frac{1}{4}x^2+\frac{1}{64}x^4-\cdots. \tag{59}$$

Therefore, the effective electric field experienced by the ion guiding center is given by further averaging (average of the average) along the Larmor orbit which yields [13 Sato]

$$E_{\perp eff} = E_0 J_0^2(k_\perp\rho)e^{i\mathbf{k}_\perp\cdot\mathbf{r}_g}. \tag{60}$$

Averaging over the velocity with Maxwellian weighting, we find the effective electric field experienced by the ion fluid,

$$E_{\perp eff} = E_0 e^{i\mathbf{k}\cdot\mathbf{r}_g}e^{-b_i}I_0(b_i), \tag{61}$$

where

$$b_i = (k_\perp\rho_i)^2 = k_\perp^2\frac{T_i/m_i}{\omega_{ci}^2}, \tag{62}$$

and use is made of the formula,

$$\int_0^\infty e^{-x^2/2}J_0^2(k_\perp\rho_i x)\,xdx = e^{-b_i}I_0(b_i). \tag{63}$$

In the long wavelength limit $b_i \ll 1$, the function $e^{-b_i} I_0 (b_i)$ approaches $1 - b_i$, and we find the effective electric field experienced by the ion guiding center

$$E_{\perp eff} \simeq E_0 \left[1 - (k_\perp \rho_i)^2\right] e^{i\mathbf{k}\cdot\mathbf{r}_g}. \tag{64}$$

The $E \times B$ drift of ions is thus modified as

$$\mathbf{v}_E = \left[1 - (k_\perp \rho_i)^2\right] \frac{\mathbf{B} \times \boldsymbol{\nabla}\phi}{B^2}, \ (k_\perp \rho_i)^2 \ll 1. \tag{65}$$

Note that the correction to the $E \times B$ drift is proportional T_i/B^3,

$$-c\frac{\mathbf{B} \times \boldsymbol{\nabla}\phi}{B^2}(k_\perp \rho_i)^2 \propto \frac{T_i}{B^3}.$$

Therefore, any other higher order ion drift up to order $1/B^3$ should be retained to be consistent. As shown earlier, the ion polarization drift

$$\mathbf{v}_{pi} = \frac{e}{m_i \omega_{ci}^2}\frac{d}{dt}\mathbf{E}_\perp, \tag{66}$$

is of order $1/B^2$, and introduces a correction to the dispersion relation similar to the finite ion Larmor radius correction. Incorporating the effective $E \times B$ drift and ion polarization drift in the ion continuity equation, we obtain

$$\frac{\partial n_i}{\partial t} + \boldsymbol{\nabla} \cdot \left[n_0 \mathbf{v}_E (1 - k_\perp^2 \rho_i^2)\right] + n_0 \boldsymbol{\nabla} \cdot \mathbf{v}_{pi} + n_0 \boldsymbol{\nabla} \cdot \mathbf{v}_\parallel = 0, \tag{67}$$

where $\mathbf{v}_\parallel$ is the ion velocity perturbation along the magnetic field. We ignore $\mathbf{v}_\parallel$ for now, but will consider it later in nonlocal analysis. The $E \times B$ drift is incompressible in a uniform plasma,

$$\boldsymbol{\nabla} \cdot \mathbf{v}_E = 0, \ \text{uniform } B. \tag{68}$$

In this case, the ion density perturbation is given by

$$\begin{aligned} n_i &= \frac{\omega_{*i} - [\omega + (1+\eta_i)\,\omega_{*i}]k_\perp^2 \rho_i^2}{\omega}\frac{e\phi}{T_i} n_0 \\ &= \frac{\omega_{*e} - [\omega + (1+\eta_i)\,\omega_{*i}]k_\perp^2 \rho_s^2}{\omega}\frac{e\phi}{T_e} n_0, \end{aligned} \tag{69}$$

where

$$\eta_i = \frac{d\ln T_i}{d\ln n_0}, \tag{70}$$

is the ion temperature gradient parameter. From charge neutrality condition $n_i = n_e = (e\phi/T_e)\, n_0$, we find

$$\omega = \frac{1 - (1+\eta_i)(k_\perp \rho_i)^2}{1 + (k_\perp \rho_s)^2}\omega_{*e}, \tag{71}$$

It should be noted that in a plasma with $T_i \simeq T_e$, the dispersion relation is valid only if $(k_\perp \rho_i)^2 \simeq (k_\perp \rho_s)^2 \ll 1$, that is, if the ion Larmor radius is sufficiently small compared with the cross-field wavelength. For arbitrary $(k_\perp \rho_i)^2$, kinetic theory must be used.

The ion flow along the magnetic field $v_\parallel$ in the continuity equation may be implemented as follows. The ion equation of motion along the magnetic field is

$$n_0 m_i \frac{\partial v_{i\parallel}}{\partial t} = n_0 e E_\parallel - \frac{\partial p_i}{\partial z}, \tag{72}$$

where $E_\parallel = -ik_\parallel \phi$ and p_i is the ion pressure perturbation which approximately obeys the convection equation,

$$\frac{\partial p_i}{\partial t} + \mathbf{v}_{E\times B} \cdot \nabla p_{i0} = 0. \tag{73}$$

Then the ion density perturbation in long wavelength limit $(k_\perp \rho_s)^2 \ll 1$ becomes

$$n_i = \left(\frac{\omega_{*e}}{\omega} + \frac{(1+\eta_i)\,\omega_{*i}\omega_s^2}{\omega^3} \right) \frac{e\phi}{T_e} n_0, \tag{74}$$

where $\omega_s = k_\parallel c_s$ is the ion acoustic transit frequency. In the limit of large η_i, we thus obtain the following dispersion relation,

$$\omega^3 \simeq \eta_i \omega_{*i} \omega_s^2, \tag{75}$$

which has an unstable solution. This ITG instability in slab geometry was found by Rudakov and Sagdeev [14]. In toroidal geometry, a toroidicity induced ITG mode with a larger growth rate prevails.

5 Drift Mode in Tokamaks

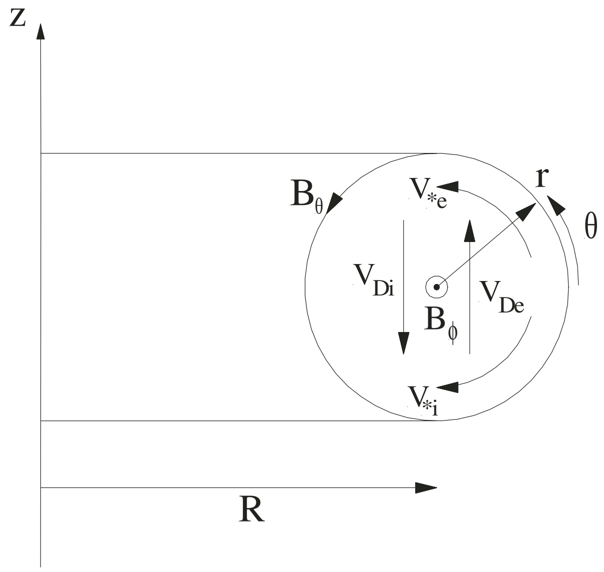

Fig. 2. Tokamak geometry. The toroidal magnetic field is nonuniform $B_\phi \propto 1/\left(R + r\cos\theta\right)$ which causes magnetic drifts of ions V_{Di} (downward) and electrons V_{De} (upward).

The basic geometry of a tokamak discharge is shown in Fig. 2. For simplicity we assume each magnetic surface is circular but they may not be concentric. In addition to the toroidal magnetic field B_ϕ,which is nonuniform and curved with a curvature radius R, the toroidal plasma current $J_{\phi 0}$, which is driven externally, creates a poloidal azimuthal magnetic field B_θ.The safety factor q against the MHD kink instability is defined by

$$q\left(r\right) = \frac{rB_\phi}{RB_\theta}, \tag{76}$$

and the magnetic shear parameter by

$$s\left(r\right) = \frac{r}{q}\frac{dq}{dr}. \tag{77}$$

s can be positive or negative depending on the radial profile of the toroidal current. The total magnetic field is helical. The poloidal magnetic field B_θ provides the rotational transform which is essential for magnetic confinement in toroidal geometry. (Recall that a simple toroidal field B_ϕ alone cannot confine charged particles.)

The gradient in the toroidal magnetic field causes guiding center drifts of both electrons and ions. In a low β plasma, the gradient and curvature drifts can be combined as

$$\mathbf{V}_{De}\left(\mathbf{v}\right) = \frac{\nabla B \times \mathbf{B}}{eB^3} m_e \left(\frac{1}{2}v_\perp^2 + v_\parallel^2\right) = m_e \left(\frac{1}{2}v_\perp^2 + v_\parallel^2\right)\frac{1}{eBR}\mathbf{e}_z, \tag{78}$$

$$\mathbf{V}_{Di}(\mathbf{v}) = \frac{\mathbf{B}\times\nabla B}{eB^3} m_i \left(\frac{1}{2}v_\perp^2 + v_\parallel^2\right) = -m_i \left(\frac{1}{2}v_\perp^2 + v_\parallel^2\right) \frac{1}{eBR}\mathbf{e}_z. \tag{79}$$

These drift velocities are shown in Fig. 2. Also shown are the electron and ion diamagnetic drift velocities V_{*e} and V_{*i} in the θ direction. Note that in the region $\theta = 0$ (the outermost region), V_{De} and V_{*e} are both upward, and V_{Di} and V_{*i} are both downward. In the region where the pressure gradient drift and magnetic curvature drift are in the same direction, the plasma is vulnerable to flute type or ballooning type instabilities.

In toroidal geometry, the divergence of the diamagnetic current is nonvanishing,

$$\nabla\cdot\mathbf{J}_* = -\frac{2}{B^3}\nabla B\cdot(\mathbf{B}\times\nabla p). \tag{80}$$

To maintain charge neutrality $\nabla\cdot\mathbf{J} = 0$, $\nabla\cdot\mathbf{J}_*$ must be compensated for by a current parallel to the magnetic field,

$$\nabla\cdot\mathbf{J}_\parallel = \frac{1}{qR}\frac{\partial J_\parallel}{\partial\theta} = \frac{2}{B^3}\nabla B\cdot(\mathbf{B}\times\nabla p) = -\frac{2}{BR}\left|\frac{dp}{dr}\right|\sin\theta, \tag{81}$$

$$J_{\parallel PS} \simeq J_\phi = \frac{2q}{B}\left|\frac{dp}{dr}\right|\cos\theta. \tag{82}$$

Therefore, in tokamaks, an extra toroidal current exists in addition to that externally driven, $J_{\phi 0}$, which creates the poloidal magnetic field B_θ. The parallel current in Eq. (82) is called Pfirsch-Schlüter current. The ratio between the magnitude of the Pfirsch-Schlüter current and $J_{\phi 0}$ is approximately given by

$$\alpha = \frac{2q}{B}\left|\frac{dp}{dr}\right|\frac{\mu_0 r}{B_\theta} = q^2 R\left|\frac{d\beta}{dr}\right|, \tag{83}$$

which is called the ballooning parameter. The poloidal magnetic field B_θ is accordingly modified as

$$B_\theta(r,\theta) \simeq B_{\theta 0}(r)(1 + \alpha(r)\cos\theta), \tag{84}$$

where $B_{\theta 0}$ is the lowest order poloidal magnetic field

$$B_{\theta 0} = \frac{\mu_0}{r}\int_0^r J_{\phi 0}(r)\, r dr. \tag{85}$$

α is related to the Shafranov shift of the magnetic axis Δ, $\alpha \simeq d\Delta/dr$. The shift is illustrated in Fig. 3.

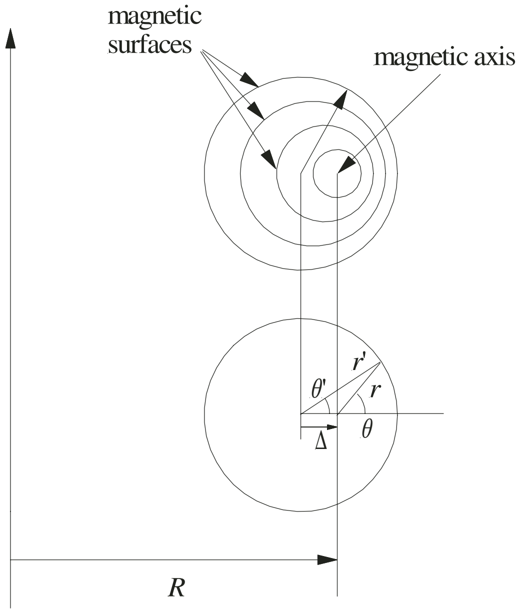

Fig. 3. Eccentric magnetic surfaces resulting from the shift of the magnetic axis on which $B_\theta = 0$. The coordinates (r, θ) pertain to the origin chosen at the magnetic axis, while (r', θ') to the center of a circular magnetic surface. They are related through $r' = r + \Delta \sin\theta'$, and $\theta = \theta' + \Delta \sin\theta / r$.

Likewise, in toroidal geometry, the magnetic curvature/gradient makes the cross-field $E \times B$ drift compressible,

$$\boldsymbol{\nabla} \cdot \mathbf{v}_E = -\frac{2\boldsymbol{\nabla} B}{B^3} \cdot (\mathbf{B} \times \boldsymbol{\nabla}\phi) \neq 0, \tag{86}$$

in contrast to the slab geometry with straight magnetic field lines. The guiding center ion magnetic drift,

$$\mathbf{V}_{Di} = -\frac{2T_i}{eBR}\mathbf{e}_z, \tag{87}$$

also enters the continuity equation. Furthermore, trapped electrons make electron response non-Boltzmann (nonadiabatic) and provide a source of strong destabilization for the drift mode. Another important toroidicity effect is the absence of stabilizing ion Landau damping in modes propagating in the electron diamagnetic drift ($\omega > 0$). This follows from the condition of ion kinetic resonance as given by

$$\omega + \omega_{Di} - k_\parallel v_\parallel = \omega + \frac{m_i}{eB^3}\left(\frac{1}{2}v_\perp^2 + v_\parallel^2\right)(\nabla B \times \mathbf{B}) \cdot \mathbf{k} - k_\parallel v_\parallel = 0, \tag{88}$$

where ω_{Di} is the velocity dependent ion magnetic drift frequency. When $\omega > 0$, the domain in the velocity space that satisfies the resonance condition is extremely narrow or even nullified, depending on the finite ion Larmor radius parameter, $k_\perp \rho_i$.

Noting that the $E \times B$ drift is compressible and incorporating the ion magnetic drift velocity and ion velocity perturbation parallel to the magnetic field, the ion continuity equation now takes the form

$$\left(\frac{\partial}{\partial t} + \mathbf{V}_{Di} \cdot \nabla\right) n_i + \boldsymbol{\nabla} \cdot \left[n_0 \mathbf{v}_E (1 - k_\perp^2 \rho_i^2)\right] + n_0 \boldsymbol{\nabla} \cdot \mathbf{v}_{pi} + n_0 \boldsymbol{\nabla} \cdot \mathbf{v}_{i\parallel} = 0. \tag{89}$$

Here

$$\mathbf{V}_{Di} = \frac{2T_i}{eB^3} \mathbf{B} \times \nabla B, \tag{90}$$

is the thermal ion magnetic drift, and $\mathbf{v}_{\parallel i}$ is the parallel velocity associated with the ion acoustic mode to be determined from the momentum balance along the magnetic field,

$$n_0 m_i \left(\frac{\partial}{\partial t} + \mathbf{V}_{Di} \cdot \boldsymbol{\nabla}\right) \mathbf{v}_{\parallel i} = -n_0 e \nabla_\parallel \phi - \nabla_\parallel p_i, \tag{91}$$

where p_i is the ion pressure perturbation. The ion polarization drift is to be evaluated with the substantive derivative,

$$\mathbf{v}_{pi} = \frac{e}{m_i \omega_{ci}^2} \left(\frac{\partial}{\partial t} + \mathbf{V}_{Di} \cdot \boldsymbol{\nabla}\right) (-\nabla_\perp \phi). \tag{92}$$

It is noted that these equations are, strictly speaking, valid if the ion temperature gradient (η_i) is negligibly small. When η_i is large, the perturbation in the ion temperature (and thus in the ion magnetic drift) must be considered. The ion temperature gradient mode (η_i mode) will be discussed separately. For now, we ignore η_i, and approximate the ion pressure perturbation by

$$p_i = T_i n_i. \tag{93}$$

Then,

$$v_{\parallel i} = \frac{e}{m_i} \frac{k_\parallel}{\omega + \omega_{Di}} \phi + \frac{T_i}{m_i} \frac{k_\parallel}{\omega + \omega_{Di}} \frac{n_i}{n_0}, \tag{94}$$

where

$$k_\parallel = \frac{1}{qR}(m - nq) - \frac{i}{qR}\frac{\partial}{\partial \theta},$$

is the gradient along the magnetic field in the tokamak magnetic geometry. Here θ is now understood to be the poloidal angle along the helical magnetic field which extends from $-\infty$ to ∞ unless on a rational magnetic surface. Substituting this into Eq. (89), and noting the cancellation between the following two terms,

$$-(k_\perp \rho_i)^2 \nabla \cdot \mathbf{v}_E - \frac{e}{m_i \omega_{ci}^2} (\mathbf{V}_{Di} \cdot \nabla) \nabla_\perp^2 \phi = 0, \tag{95}$$

we obtain for n_i

$$\left(\omega+\omega_{Di}-\frac{1}{\tau}c_s^2 k_\parallel \frac{1}{\omega+\omega_{Di}}k_\parallel\right)n_i=\left\{\omega_{*e}-\omega_{De}-(\omega+\omega_{*i})(k_\perp\rho_s)^2+c_s^2 k_\parallel\frac{1}{\omega+\omega_{Di}}k_\parallel\right\}\frac{e\phi}{T_e}n_0, \tag{96}$$

where $\tau = T_e/T_i$ is the temperature ratio, and $c_s = \sqrt{T_e/M}$ is the ion acoustic speed. It is noted that the differential operator $k_\parallel$ operates on $\omega_{Di}(\theta)$ and $b_s(\theta)$ as well as on n_i and ϕ where θ is the extended poloidal angle. The perturbation is assumed to be in the form $f(\theta)\, e^{i(m\theta-n\phi)}$ where ϕ is the toroidal angle. Near a rational surface where $m = nq$ with m and n being integers, the cross field differential operator becomes

$$\nabla_\perp e^{inq(r)\theta(r)}=i\frac{nq}{r}\mathbf{e}_\theta+in\left(\frac{dq}{dr}\theta+q\frac{d\theta}{dr}\right)\mathbf{e}_r=k_\theta\left[\mathbf{e}_\theta+(s\theta-\alpha\sin\theta)\,\mathbf{e}_r\right], \tag{97}$$

where $k_\theta = m/r$ and use is made of

$$\frac{d\theta}{dr}\simeq-\frac{1}{r}\frac{d\Delta}{dr}\sin\theta=-\frac{\alpha}{r}\sin\theta.$$

(See Fig. 3.) Therefore,

$$k_\perp^2=k_\theta^2\left[1+(s\theta-\alpha\sin\theta)^2\right]. \tag{98}$$

Likewise,

$$\omega_D=\mathbf{k}\cdot\mathbf{V}_D=\frac{2T}{eBR}k_\theta\left[\mathbf{e}_\theta+(s\theta-\alpha\sin\theta)\,\mathbf{e}_r\right]\cdot\mathbf{e}_z=2\varepsilon_n\omega_*\left[\cos\theta+(s\theta-\alpha\sin\theta)\sin\theta\right], \tag{99}$$

where $\varepsilon_n = L_n/R$.

The density perturbation of electrons may be found from the integral of the kinetic equation,

$$f_e=\frac{e\phi}{T_e}f_{Me}-\frac{\omega-\omega_{*e}\left(v^2\right)}{\omega-\omega_{De}\left(\mathbf{v}\right)-k_\parallel v_\parallel}\frac{e\phi}{T_e}f_{Me}, \tag{100}$$

where

$$\omega_{*e}\left(v^2\right)=\omega_{*e}\left[1+\eta_e\left(\frac{m_e v^2}{2T_e}-\frac{3}{2}\right)\right], \tag{101}$$

in the energy dependent diamagnetic drift frequency. An approximate electron density pertubation is

$$n_e\simeq\left(1-\sqrt{2\epsilon}\,\frac{(\omega-\frac{7}{3}\omega_{Det})(\omega-\omega_{*e})-\eta_e\omega_{*e}\omega_{Det}}{(\omega-\frac{5}{3}\omega_{Det})^2-\frac{10}{9}\omega_{Det}^2}\right)\frac{e\phi}{T_e}n_0, \tag{102}$$

where

$$\omega_{Det} = \frac{T_e}{eB^3} (\nabla B \times \mathbf{B}) \cdot \mathbf{k} = \frac{1}{2} \omega_{De},$$

is the magnetic drift frequency of trapped electrons satisfying $\varepsilon v_\perp^2 > v_\parallel^2$. Equating the electron density to the ion density in Eq. (96), we obtain the following mode equation,

$$\left(\frac{c_s}{qR}\right)^2 \frac{d}{d\theta} \left\{ \frac{1}{\omega + \omega_D} \frac{d}{d\theta} \frac{\phi}{\omega + \omega_D} \right\} + V(\theta)\phi = 0, \tag{103}$$

where

$$V(\theta) = \frac{1}{1 + F_e} \left(F_e - \frac{\omega_* - \omega_D(\theta) - (\omega + \omega_*) b(\theta)}{\omega + \omega_D(\theta)} \right), \tag{104}$$

$$F_e = 1 - \sqrt{2\epsilon} \frac{(\omega - \frac{7}{6}\omega_D)(\omega - \omega_*) - \frac{1}{2}\eta_e \omega_* \omega_D}{(\omega - \frac{5}{6}\omega_D)^2 - \frac{5}{18}\omega_D^2}, \tag{105}$$

$$b(\theta) = (k_\theta \rho)^2 \left[1 + (s\theta - \alpha \sin\theta)^2 \right]. \tag{106}$$

and $T_i = T_e$ has been assumed.

Equation (103) can be solved numerically with a complex shooting code. Fig. 4 shows the dispersion relation, $(\omega_r + i\gamma)/c_s/L_n$ vs. $b_0 = (k_\theta \rho)^2$ when $\alpha = 0, \epsilon_n = L_n/R = 0.4$, $\epsilon = r/R = 0.25$, $\eta_e = 1$, $s = 1$, $q = 2$. At $b_0 = 0.01$, the eigenvalue is $(\omega_r + i\gamma)/c_s/L_n \simeq 0.12 + i0.04$. In the long wavelength regime, $(k_\theta \rho)^2 \simeq 0.01$, coupling to the ion acoustic mode is evident since $\omega_r/\omega_s = \omega_r/(c_s/qR)$ is of order unity. However, in toroidal geometry, ion Landau damping is practically absent, and the ion acoustic mode can be unstable being driven by the trapped electrons. It is noted that the electron temperature gradient has a destabilizing influence because the instability is driven by the interchange effect associated with the trapped electrons. Also it has been found that electromagnetic (finite β) effects are destabilizing in contrast to the ion temperature gradient (ITG) mode, which will be discussed in the following Section.

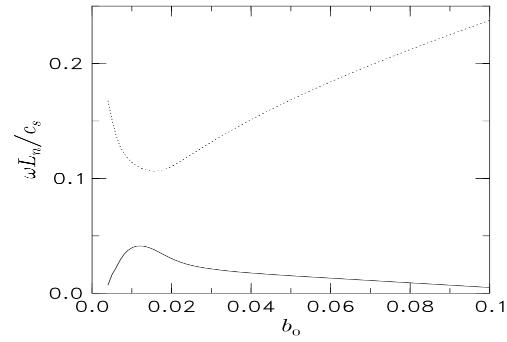

Fig. 4. Normalized frequency $\omega_r L_n/c_s$ (dotted line) and growth rate $\gamma L_n/c_s$ (solid line) of the collisionless trapped electron drift mode *vs.* $b_0 = (k_\theta \rho)^2$.

6 Toroidal Ion Temperature Gradient Mode

In toroidal geometry with magnetic shear, the η_i mode is driven largely by the interchange effect through the coupling of the ion pressure gradient with the unfavorable magnetic curvature. Jarmén *et al.* [8] have made a detailed study on the toroidal η_i mode within the hydrodynamic approximation,

$$(k_\perp \rho_i)^2 \ll 1, \ \omega + \omega_{Di} \gg k_\parallel c_s. \tag{107}$$

In the analysis by Jarmén *et al.*, the ion pressure perturbation has been obtained from the Braginskii heat balance equation

$$\frac{3}{2}\frac{\partial p_i}{\partial t} + \frac{3}{2}\boldsymbol{\nabla}\cdot(p_i \mathbf{V}) + p_i \boldsymbol{\nabla}\cdot\mathbf{V} + \boldsymbol{\nabla}\cdot\mathbf{q}_i = 0, \tag{108}$$

where p_i is the ion pressure, $\mathbf{V}$ is the ion fluid velocity, and $\mathbf{q}_i$ is the cross field ion heat flux,

$$\mathbf{q}_i = \frac{5}{2}\frac{p_i}{eB^2}\mathbf{B}\times\boldsymbol{\nabla}T_i. \tag{109}$$

The divergence of $\mathbf{q}_i$ is

$$\boldsymbol{\nabla}\cdot\mathbf{q}_i = -\frac{5}{2}n\left(\mathbf{V}_{*i} - \mathbf{V}_{Di}\right)\cdot\boldsymbol{\nabla}T_{i,} \tag{110}$$

where

$$\mathbf{V}_{*i} = \frac{\mathbf{B}\times\nabla p_i}{neB^2}, \tag{111}$$

is the ion diamagnetic drift velocity, and

$$\mathbf{V}_{Di} = \frac{2p_i}{neB^3}\mathbf{B}\times\nabla B, \tag{112}$$

is the ion magnetic drift velocity. Linearization of Eq. (108) by assuming

$$p_i = p_{i0} + \widetilde{p}_i$$

yields

$$\frac{3}{2}\left(\frac{\partial}{\partial t} + \tfrac{5}{3}\mathbf{V}_{Di}\cdot\nabla\right)\widetilde{p}_i - \frac{5}{2}T_i\left(\frac{\partial}{\partial t} + \mathbf{V}_{Di}\cdot\nabla\right)n_i - \mathbf{v}_E\cdot\left(T_i\nabla n - \frac{3}{2}n\nabla T_i\right) = 0, \tag{113}$$

or

$$\widetilde{p}_i = \frac{5}{3}\frac{\omega + \omega_{Di}}{\omega + \frac{5}{3}\omega_{Di}}T_i n_i + \frac{\omega_{*i}}{\omega + \frac{5}{3}\omega_{Di}}\left(\eta_i - \frac{2}{3}\right)n_0 e\phi. \tag{114}$$

The perturbed ion diamagnetic current is thus given by

$$\mathbf{J}_{*i} = \frac{\mathbf{B}\times\boldsymbol{\nabla}\widetilde{p}_i}{B^2}.$$

Substituting this into the ion continuity equation,

$$\frac{\partial n_i}{\partial t} + \frac{1}{e}\boldsymbol{\nabla}\cdot\mathbf{J}_{*i} + \boldsymbol{\nabla}\cdot\left\{\mathbf{v}_E[1-(k_\perp\rho_i)^2]n_0\right\} + n_0\nabla\cdot\mathbf{v}_{pi} = 0, \tag{115}$$

where $\mathbf{v}_E[1-(k_\perp\rho_i)^2]$ is the ion $E\times B$ drift corrected for the finite ion Larmor radius effect, and $\bar{v}_{pi}$ is the ion polarization drift,

$$\mathbf{v}_{pi} = \frac{e}{m_i\omega_{ci}^2}\left(\frac{\partial}{\partial t} + \mathbf{V}_{Di}\cdot\nabla\right)(-\nabla_\perp\phi), \tag{116}$$

we readily find the ion density perturbation in terms of the potential ϕ,

$$n_i = \frac{\left(\omega + \frac{5}{3}\omega_{Di}\right)\left\{\omega_{*e} - \omega_{De} - \left[\omega + \omega_{*i}(1+\eta_i)\right](k_\perp\rho)^2\right\} - \left(\eta_i - \frac{2}{3}\right)\omega_{*e}\omega_{Di}}{\left(\omega + \frac{5}{3}\omega_{Di}\right)^2 - \frac{10}{9}\omega_{Di}^2}\frac{e\phi}{T_e}n_0. \tag{117}$$

This result qualitatively agrees with the ion density perturbation derived from the gyro-kinetic analysis,

$$n_i = -\frac{e\phi}{T_i}n_0 + \left\langle\frac{\omega + \widehat{\omega}_{*i}(v^2)}{\omega + \widehat{\omega}_{Di}(\mathbf{v}) - k_\parallel v_\parallel}J_0^2\left(\frac{k_\perp v_\perp}{\omega_{ci}}\right)\right\rangle_{\mathbf{v}}\frac{e\phi}{T_i}n_0, \tag{118}$$

provided the ion transit effect $\left(k_{\parallel}v_{\parallel}\right)$ is negligibly small. The ion magnetic drift frequency ω_{Di} plays double roles, one to cause a guiding center drift which is destabilizing through the interchange affect $(\omega_{*e}\omega_{Di})$ and another to cause a thermal spread ($-\omega_{Di}^2$ term in the denominator) which is stabilizing.

If the trapped electrons are ignored, the electron density perturbation is Boltzmann,

$$n_e = \frac{e\phi}{T_e} n_0.$$

The charge neutrality condition $n_i = n_e$ thus yields a dispersion relation which is quadratic in ω and the condition for the instability is given by

$$\eta_i > \frac{2}{3} + \frac{1}{4}\frac{\left(\omega_{*e} - \omega_{De}\right)^2 + \frac{10}{9}\omega_{Di}^2}{\omega_{*e}\omega_{Di}}. \tag{119}$$

Approximating $\omega_{De} = 2\varepsilon_n \omega_{*e}$ and $\omega_{Di} = 2\varepsilon_n \omega_{*i}$, we find

$$\eta_i > \frac{2}{3} + \frac{1}{4}\frac{\left(1 - 2\varepsilon_n\right)^2 + \frac{10}{9}\left(2\varepsilon_n/\tau\right)^2}{2\varepsilon_n/\tau}, \tag{120}$$

where $\varepsilon_n = L_n/R$ and $\tau = T_e/T_i$. In the limit of flat density profile $\varepsilon_n > 1$, we find

$$\eta_i > \frac{2}{3} + \frac{1}{2}\frac{\varepsilon_n \tau^2 + \frac{10}{9}\varepsilon_n}{\tau},$$

while in the case of steep density gradient $\varepsilon_n < 1$,

$$\eta_i > \frac{2}{3} + \frac{1}{4}\left(\frac{\tau}{2\varepsilon_n} + \frac{20\varepsilon_n}{9\tau}\right).$$

Also, it is noted that the critical η_i increases as the ion temperature exceeds the electron temperature $\tau < 1$.

As is evident in Eq. (119), the main drive of the toroidal η_i mode comes from the interchange term. An approximate dispersion relation is

$$\omega^2 \simeq -\left(\eta_i - \eta_c\right)\omega_{*i}\omega_{De}, \tag{121}$$

where $\eta_c \simeq 1$ is the critical ion temperature gradient. Trapped electrons further destabilize the ITG mode [9],

$$\omega^2 \simeq -\left(\eta_i - \eta_c\right)\omega_{*i}\omega_{De} - \sqrt{2\varepsilon}\eta_e \omega_{*e}\omega_{Det}, \tag{122}$$

However, the toroidal ITG mode is subject to effective stabilization by a finite β [9].

7 Local Kinetic Formulation for Electrostatic Modes

When kinetic resonance (Landau damping) is important, and one of the basic assumptions of hydrodynamic approximation, $(k_\perp \rho)^2 \ll 1$, becomes dubious, one has to resort to the kinetic analysis based on the Vlasov equation for the velocity distribution function f,

$$\frac{\partial f}{\partial t} + \mathbf{v} \cdot \boldsymbol{\nabla} f + \frac{e}{m} (\mathbf{E} + \mathbf{v} \times \mathbf{B}) \cdot \frac{\partial f}{\partial \mathbf{v}} = 0, \tag{123}$$

and then evaluate the density perturbation from

$$n = \int f d^3 v. \tag{124}$$

For low-frequency, drift-type modes with $\omega \ll \omega_{ci}$ ($\ll \omega_{ce}$), the effects of higher harmonics of the ion cyclotron frequency may be ignored.

In this Section, a procedure is outlined to solve the Vlasov equation for electrostatic modes, described by $\mathbf{E}_1 = -\nabla\phi$, $\mathbf{B}_1 = 0$ (negligible magnetic perturbation). Linearizing Eq. (123) with $f = f_0 + f_1$ and singling out the $E \times B$ drift velocity, we obtain

$$\frac{df_1}{dt} + \mathbf{v}_E \cdot \boldsymbol{\nabla} f_0 - \frac{e}{m} \boldsymbol{\nabla}\phi \cdot \frac{\partial f_0(v^2, \mathbf{x})}{\partial \mathbf{v}} = 0, \tag{125}$$

where

$$\frac{d}{dt} = \frac{\partial}{\partial t} + \mathbf{v} \cdot \boldsymbol{\nabla} + \frac{e}{m} (\mathbf{v} \times \mathbf{B}) \cdot \frac{\partial}{\partial \mathbf{v}}, \tag{126}$$

is the substantive derivative along the unperturbed particle trajectory determined from the equation of motion

$$m \frac{d\mathbf{v}}{dt} = e\mathbf{v} \times \mathbf{B}, \ \mathbf{v} = \frac{d\mathbf{r}}{dt}. \tag{127}$$

It is noted that the $E \times B$ drift term actually stems from the velocity derivative pertinent to a nonuniform plasma in which the unperturbed distribution function f_0 can be a function of the canonical momentum,

$$\mathbf{r}_\perp - \frac{\boldsymbol{\omega}_c \times \mathbf{v}_\perp}{\omega_c^2}, \tag{128}$$

as well as the energy. (Strictly speaking, this quantity is an invariant only in a uniform magnetic field and in nonuniform magnetic field, it is only approximately an invariant.) Nonuniformity in the magnetic field introduces the magnetic drift,

$$\mathbf{V}_D = \frac{m}{eB^3} \left(\frac{1}{2} v_\perp^2 + v_\parallel^2 \right) \mathbf{B} \times \nabla B, \tag{129}$$

which can be implemented in the analysis as an effective Doppler shift. The velocity derivative can be performed as follows:

$$\frac{\partial}{\partial \mathbf{v}} f_0 \left(v^2,\ \mathbf{r}_\perp - \frac{\boldsymbol{\omega}_c \times \mathbf{v}_\perp}{\omega_c^2} \right) \simeq \frac{\partial f_0(v^2)}{\partial \mathbf{v}} + \frac{1}{\omega_c^2} \boldsymbol{\omega}_c \times \nabla f_0.$$

Then,

$$-\frac{e}{m} \nabla \phi \cdot \left(\frac{\partial f_0(v^2)}{\partial \mathbf{v}} + \frac{1}{\omega_c^2} \boldsymbol{\omega}_c \times \nabla f_0 \right) = -\frac{e}{m} \nabla \phi \cdot \frac{\partial f_0(v^2)}{\partial \mathbf{v}} + \mathbf{v}_E \cdot \nabla f_0,$$

where

$$\mathbf{v}_E = \frac{\mathbf{B} \times \nabla \phi}{B^2},$$

is the $E \times B$ drift.

If the unperturbed distribution $f_0(\mathbf{v})$ is assumed to be Maxwellian, $f_M(v^2)$, which is reasonable provided the confinement time far exceeds the collision time, the velocity derivative becomes

$$\frac{\partial f_0}{\partial \mathbf{v}} = -\frac{m\mathbf{v}}{T} f_M. \tag{130}$$

Assuming all perturbations are proportional to $e^{i(\mathbf{k}\cdot\mathbf{r}-\omega t)}$, and noting

$$\frac{e}{m} (\mathbf{v} \times \mathbf{B}) \cdot \frac{\partial}{\partial \mathbf{v}} = -\omega_c \frac{\partial}{\partial \alpha}, \tag{131}$$

where

$$\alpha = \tan^{-1} \left(\frac{v_y}{v_x} \right), \tag{132}$$

is the gyroangle, we may reduce Eq. (125) to

$$\omega_c \frac{\partial f}{\partial \alpha} + i \left(\omega - \mathbf{k} \cdot \mathbf{V}_D - \mathbf{k} \cdot \mathbf{v} \right) f - \mathbf{v}_E \cdot \boldsymbol{\nabla} f_M - \frac{e}{T} \left(\mathbf{v} + \mathbf{V}_D \right) \cdot \boldsymbol{\nabla} \phi f_M = 0, \tag{133}$$

where $\mathbf{V}_D$ is the velocity dependent magnetic drift velocity and $\mathbf{v}$ is the random velocity. The part of f independent of the gyroangle α can be singled out as

$$f = -\frac{e\phi}{T} f_M + g,$$

where g satisfies

$$\omega_c \frac{\partial g}{\partial \alpha} + i \left(\omega - \mathbf{k} \cdot \mathbf{V}_D - \mathbf{k} \cdot \mathbf{v} \right) g - \mathbf{v}_E \cdot \boldsymbol{\nabla} f_M + i\omega \frac{e\phi}{T} f_M = 0.$$

If $\mathbf{k}$ is chosen to be $\mathbf{k} = k_\perp \mathbf{e}_x + k_\parallel \mathbf{e}_z$, we have $\mathbf{k} \cdot \mathbf{v} = k_\perp v_\perp \cos\alpha + k_\parallel v_\parallel$. Solving for g is effected by using the expansion,

$$e^{\pm ix \sin\alpha} = \sum_{m=-\infty}^{\infty} J_m(x) e^{\pm im\alpha}, \tag{134}$$

twice with the result

$$\begin{aligned} f &= -\frac{e\phi}{T}f_M + \sum_{m,n} J_m\left(\frac{k_\perp v_\perp}{\omega_c}\right) J_n\left(\frac{k_\perp v_\perp}{\omega_c}\right) e^{i(m-n)\alpha} \frac{\omega - \hat{\omega}_*}{\omega - \mathbf{k}\cdot\mathbf{V}_D - k_\parallel v_\parallel - n\omega_c}\frac{e\phi}{T}f_M \\ &\simeq -\frac{e\phi}{T}f_M + \frac{\omega - \hat{\omega}_*}{\omega - \mathbf{k}\cdot\mathbf{V}_D - k_\parallel v_\parallel} J_0^2\left(\frac{k_\perp v_\perp}{\omega_c}\right)\frac{e\phi}{T}f_M, \end{aligned} \tag{135}$$

where $\omega \ll \omega_c$ is recalled and

$$\widehat{\omega}_*(v^2) = \frac{T}{eB^2}(\mathbf{B}\times\nabla \ln f_M)\cdot\mathbf{k} = \frac{T}{eB^2}(\mathbf{B}\times\nabla\ln n_0)\cdot\mathbf{k}\left[1+\eta\left(\frac{mv^2}{2T}-\frac{3}{2}\right)\right], \tag{136}$$

$$\mathbf{k}\cdot\mathbf{V}_D = \frac{m}{eB^3}\left(\frac{1}{2}v_\perp^2 + v_\parallel^2\right)(\mathbf{B}\times\ln B)\cdot\mathbf{k}. \tag{137}$$

For ions, we define the energy dependent diamagnetic frequency by

$$\widehat{\omega}_{*i}(v^2) = \omega_{*i}\left[1+\eta_i\left(\frac{m_i v^2}{2T_i}-\frac{3}{2}\right)\right], \tag{138}$$

where

$$\omega_{*i} = \frac{T_i}{eB^2}(\nabla\ln n\times\mathbf{B})\cdot\mathbf{k}, \tag{139}$$

and the ion magnetic drift frequency by

$$\widehat{\omega}_{Di}(\mathbf{v}) = -\mathbf{k}\cdot\mathbf{V}_{Di}(\mathbf{v}). \tag{140}$$

Then, the perturbed ion distribution function is

$$f_i = -\frac{e\phi}{T_i}f_{Mi} + \frac{\omega+\widehat{\omega}_{*i}}{\omega+\widehat{\omega}_{Di}-k_\parallel v_\parallel}J_0^2\left(\frac{k_\perp v_\perp}{\omega_{ci}}\right)\frac{e\phi}{T_i}f_{Mi}. \tag{141}$$

For electrons, with the definitions

$$\begin{aligned} \widehat{\omega}_{*e}(v^2) &= \omega_{*e}\left[1+\eta_e\left(\frac{m_e v^2}{2T_e}-\tfrac{3}{2}\right)\right], \\ \omega_{*e} &= \frac{T_e}{eB^2}(\nabla\ln n\times B)\cdot\mathbf{k}, \\ \widehat{\omega}_{De}(\mathbf{v}) &= \mathbf{k}\cdot\mathbf{V}_{De}(\mathbf{v}), \end{aligned}$$

we approximate the distribution function by

$$f_e = \frac{e\phi}{T_e}f_{Me} - \frac{\omega-\widehat{\omega}_{*e}}{\omega-\widehat{\omega}_{De}-k_\parallel v_\parallel\delta_{jU}}\frac{e\phi}{T_e}f_{Me} \tag{142}$$

where $\delta_{jU} = 0$ for trapped electrons ($j = T$, $\left|v_\parallel\right| < \sqrt{\epsilon} v_\perp$) and $\delta_{jU} = 0$ for untrapped electrons ($j = U$, $\left|v_\parallel\right| > \sqrt{\epsilon} v_\perp$). In drift-type modes, the effect of finite electron Larmor radius can be ignored. The dispersion relation (or the mode equation) is thus found from the charge neutrality,

$$\int f_i d^3 v = \int f_e d^3 v, \tag{143}$$

or

$$1 + \tau = \tau \left\langle \frac{\omega + \widehat{\omega}_{*i}(v^2)}{\omega + \widehat{\omega}_{Di}(\mathbf{v}) - k_\parallel v_\parallel} J_0^2 \left(\frac{k_\perp v_\perp}{\omega_{ci}} \right) \right\rangle_{\text{ion}} + \left\langle \frac{\omega - \widehat{\omega}_{*e}(v^2)}{\omega - \widehat{\omega}_{De}(\mathbf{v}) - k_\parallel v_\parallel \delta_{uj}} \right\rangle_{\text{electron}}, \tag{144}$$

where $\langle \cdots \rangle$ indicates averaging over the velocity with Maxwellian weighting, and $\tau = T_e/T_i$.

The kinetic dispersion relation derived in the preceding section is, strictly speaking, valid only when the norm of the differential operation $\mathbf{k}$ is known for eigenfunction $\phi(\mathbf{r})$. In tokamaks, most drift-type modes are driven by the interchange effect, and the eigenfunction is expected to peak in the unfavorable curvature region. We therefore assume a trial function [15 Coppi, 16 Hirose]

$$\phi(\theta) = \begin{cases} \dfrac{1}{\sqrt{3\pi}} (1 + \cos\theta), & |\theta| \leq \pi \\ \\ 0, & |\theta| \geq \pi \end{cases} \tag{145}$$

where θ is the extended poloidal angle along the helical magnetic field.

The norm of $k_\parallel$ can be evaluated from

$$\begin{aligned} \left\langle k_\parallel^2 \right\rangle_\theta &= -\frac{1}{(qR)^2} \int_{-\pi}^{\pi} \phi \frac{d^2\phi}{d\theta^2} \, d\theta \\ &= \frac{1}{3(qR)^2}. \end{aligned} \tag{146}$$

Since the magnetic drift frequency in the ballooning space is

$$\omega_D(\theta) = \frac{mc}{eBR} \left(\tfrac{1}{2} v_\perp^2 + v_\parallel^2 \right) k_\theta \left(\cos\theta + s\theta \sin\theta \right), \tag{147}$$

its norm is

$$\langle \omega_D \rangle_\theta = \frac{mck_\theta}{eBR} \left(\tfrac{1}{2} v_\perp^2 + v_\parallel^2 \right) \left(\tfrac{2}{3} + \tfrac{5}{9} s \right), \tag{148}$$

and similarly

$$\left\langle k_\perp^2 \right\rangle_\theta = k_\theta^2 \left[1 + \left(\tfrac{1}{3}\pi^2 - \tfrac{5}{2} \right) s^2 \right]. \tag{149}$$

Of course, for eigenfunctions that cannot be approximated by the simple trial function in Eq. (145), these norms become invalid.

Let us apply this semi-local kinetic dispersion relation to the η_i mode, for which a rigorous integral equation analysis has also been made. In Fig. 5, the growth rate found from Eq. (144) with the norms in Eqs. (146)–(149) is compared with that obtained from a kinetic integral equation code [17 Elia]

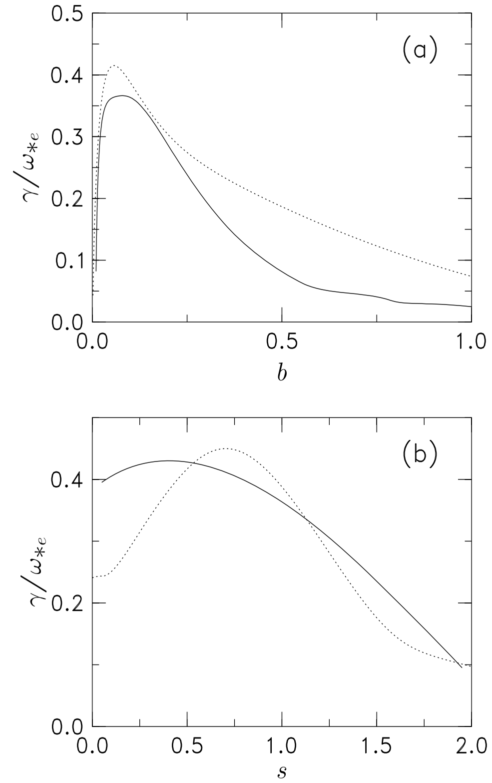

Fig. 5. (a) Growth rate γ/ω_{*e} vs. $b = (k_\theta \rho)^2$ and (b) vs. s of the toroidal ITG mode when $L_n/R = 0.1$, $\eta_i = 2$, $q = 2$. In (a), $s = 1$ and in (b), $b = 0.1$. Solid line is from local kinetic analysis and dashed line from the ballooning mode equation.

8 Effects of Magnetic Shear on the Drift Mode

In slab geometry with a sheared magnetic field

$$\mathbf{B}(r) = B\left(\frac{r}{L_s}\mathbf{e}_\theta + \mathbf{e}_z\right),$$

where r is the radial distance from a magnetic surface on which $k_{\|} = 0$, the parallel wavenumber becomes a function of the distance r,

$$k_{\|}(r) = -\frac{i}{|\mathbf{B}(r)|}\mathbf{B}(r)\cdot\nabla = k_\theta \frac{r}{L_s},$$

L_s is the magnetic shear length. Note that in slab geometry, variation along the z axis is ignored. Therefore, near the rational surface, the condition of adiabatic electron response, $\omega \ll k_{\|} v_{Te}$, may be violated. (In toroidal geometry, $k_{\|}$ remains finite even at rational surfaces, since

$$k_{\|} = \frac{1}{qR}\left(m - nq - i\frac{\partial}{\partial\theta}\right),$$

where $\partial/\partial\theta$ takes into account slow variation of amplitude of eigenfunctions with the poloidal angle θ.)

In the limit of low ion temperature $T_i \ll T_e$, the ion density perturbation is given by

$$n_i = \left[\frac{\omega_{*e}}{\omega} - (k_\perp \rho_s)^2 + \frac{(k_{\|} c_s)^2}{\omega^2}\right]\frac{e\phi}{T_e}n_0, \;\; \rho_s = \frac{c_s}{\omega_{ci}}. \tag{150}$$

The electron density perturbation is

$$n_e = \left[1 + \frac{\omega - \omega_{*e}}{\omega}\zeta_e Z(\zeta_e)\right]\frac{e\phi}{T_e}n_0, \tag{151}$$

where

$$\zeta_e = \frac{\omega}{|k_{\|}|\, v_{Te}}, \tag{152}$$

is the argument of the plasma dispersion function $Z(\zeta_e)$. Noting

$$k_\perp^2 = k_\theta^2 - \frac{\partial^2}{\partial r^2}, \tag{153}$$

we obtain from charge neutrality $n_i = n_e$ the following equation for $\phi(x)$,

$$\left[\frac{d^2}{dx^2} - (k_\theta \rho)^2 + \frac{\omega_s^2}{\omega^2}x^2 - \frac{\omega - \omega_{*e}}{\omega}\left[1 + \zeta_e Z(\zeta_e)\right]\right]\phi(x) = 0, \tag{154}$$

where $x = r/\rho_s$, $\omega_s = k_\theta \rho_s c_s / L_s$, and

$$\zeta_e = \frac{\omega\tau}{|x|}, \;\; \tau = \frac{L_s}{k_\theta \rho_s v_{Te}}. \tag{155}$$

τ is essentially the electron transit time over the shear length L_s. Eq. (154) can be solved numerically (using shooting code). No bounded unstable solutions have been found. A finite electron temperature gradient and finite ion temperature do not alter this conclusion.

However, if the drift frequency ω_{*e} is not constant but depends on r being peaked at the rational surface, an instability may set in. The case of Gaussian dependence,

$$\omega_{*e}(r) = \omega_{*0} \exp\left(-\frac{r^2}{L^2}\right), \tag{156}$$

has been analyzed by Hojo and Watanabe [18] with a conclusion that an instability can occur if the length L, which characterizes the nonuniformity in $\omega_{*e}(r)$ profile, satisfies

$$\frac{\rho}{L} > \frac{L_n}{L_s} \text{ or } \rho L_s > L L_n.$$

as demonstrated in Fig. 6. This condition is similar to that found by Krall and Rosenbluth [2], $\rho L_s > L_n^2$.

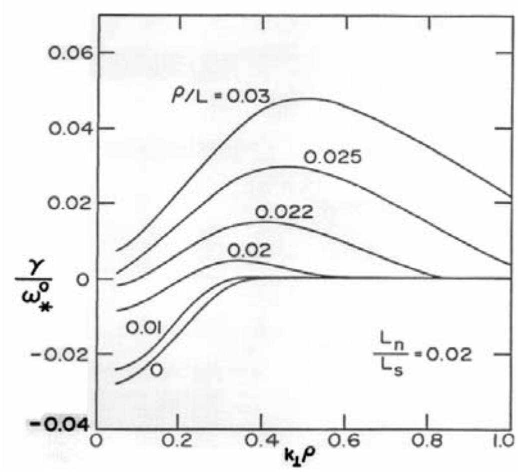

Fig. 6. Unstable drift mode in slab geometry when ω_{*e} is nonuniform. Growth rate γ/ω_{*0} vs. $k_\perp\rho$. $\tau\omega_{*0} = 1$, $L_n/L_s = 0.02$.

In tokamaks, magnetic shear s has in general destabilizing effects on drift type modes. This tendency has been observed in the toroidal ITG and ETG modes and also in the toroidicity induced drift mode. Fig. 7 shows shear dependence of the growth rate of short wavelength ITG mode. The growth rate is approximately proportional to $\sqrt{|s|}$ which indicates that finite shear, either positive or negative, is needed for the mode to be unstable. The case of ETG mode is shown in Fig. 8. In general, weak magnetic shear may be favourable for suppression of the drift modes [19, 20].

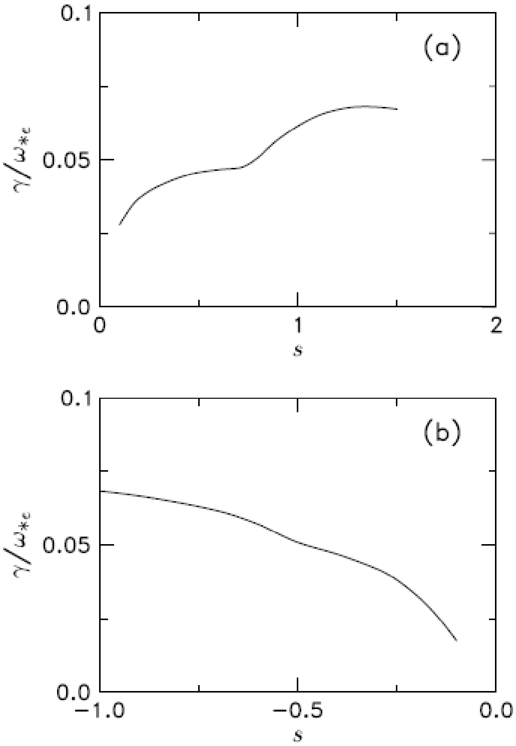

Fig. 7. Dependence of the ITG growth rate on the shear parameter s. Shear is destabilizing in both positive and negative regions.

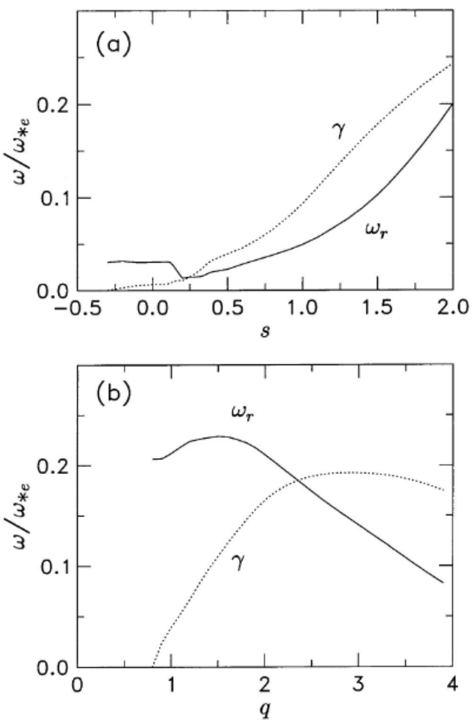

Fig. 8. (a) Mode frequency and growth rate of the ETG mode vs. shear s. (b) Dependence on the safety factor q.

9 Electromagnetic Formulation

The plasma β factor defined by

$$\beta = \frac{p}{B^2/2\mu_0},$$

is an important economic figure of merit of fusion power reactor. It is equally important in plasma stability, for some instabilities (e.g., the ballooning mode) set in if the β factor exceeds a threshold value. In drift mode analysis, the primary interest will be in whether a finite β tends to further destabilize predominantly electrostatic drift type modes, or not. In addition to the scalar potential ϕ, the parallel vector potential $A_\parallel$ enters as the second field to introduce the shear Alfven mode. (In low β plasmas, the third field $B_\parallel$ associated with the magnetosonic perturbation may still be ignored.)

The Alfven mode is characterized by magnetic field line bending which causes particle drift

$$v_\parallel \frac{\mathbf{B}_\perp}{B}. \tag{157}$$

This is still an $\mathbf{E} \times \mathbf{B}$ drift with a motional electric field given by

$$\mathbf{E}' = \mathbf{v}_\parallel \times \mathbf{B}_\perp, \tag{158}$$

which yields

$$\frac{\mathbf{E}' \times \mathbf{B}}{B^2} = v_\parallel \frac{\mathbf{B}_\perp}{B}. \tag{159}$$

Combining with the electrostatic $\mathbf{E} \times \mathbf{B}$ drift, we thus find the total perturbed drift,

$$\mathbf{v}_D = \frac{\mathbf{B} \times \boldsymbol{\nabla}\phi}{B^2} + v_\parallel \frac{\mathbf{B}_\perp}{B}. \tag{160}$$

Noting

$$\mathbf{E} = -\nabla\phi - \frac{\partial \mathbf{A}_\parallel}{\partial t}, \tag{161}$$

and following the same procedure as developed in the preceding section, we obtain

$$f = -\frac{e\phi}{T} f_M + \frac{\omega - \widehat{\omega}_*}{\omega - \widehat{\omega}_D - k_\parallel v_\parallel} \left(\phi - v_\parallel A_\parallel\right) J_0^2(\Lambda) \frac{e}{T} f_M, \tag{162}$$

with $\Lambda = k_\perp v_\perp / \omega_c$.

The basic equations to govern low frequency, long wavelength modes are the charge neutrality condition

$$n_i = n_e, \text{ or } \int f_i d\mathbf{v} = \int f_e d\mathbf{v}, \; k \ll k_D \text{ (Debye wavenumber)}, \tag{163}$$

and parallel Ampere's law,

$$\nabla_\perp^2 A_\parallel = -\mu_0 J_\parallel = -\mu_0 e \int v_\parallel (f_i - f_e) d\mathbf{v}, \tag{164}$$

where the perturbed ion distribution function f_i can be found from Eq. (162),

$$f_i = -\frac{e\phi}{T_i} f_{Mi} + \frac{\omega + \widehat{\omega}_{*i}}{\omega - k_\parallel v_\parallel + \widehat{\omega}_{Di}} J_0^2 \left(\frac{k_\perp v_\perp}{\omega_{ci}}\right) \left(\phi - v_\parallel A_\parallel\right) \frac{e}{T_i} f_{Mi}, \tag{165}$$

with

$$\widehat{\omega}_{*i}(v^2) = \frac{T_i}{eB^2}\left[1 + \eta_i \left(\frac{m_i v^2}{2T_i} - \frac{3}{2}\right)\right] [\boldsymbol{\nabla}(\ln n_0) \times \mathbf{B}_0] \cdot \mathbf{k}_\perp, \tag{166}$$

$$\widehat{\omega}_{Di}(\mathbf{v}) = \frac{m_i}{eB^3}\left(\frac{1}{2}v_\perp^2 + v_\parallel^2\right) (\boldsymbol{\nabla} B \times \mathbf{B}_0) \cdot \mathbf{k}_\perp. \tag{167}$$

We assume that the mode frequency is much larger than the ion transit frequency $|\omega| \gg k_\parallel v_{Ti}$. This is well satisfied in the toroidal ITG and ballooning modes which are our main interest. Then the ion density perturbation becomes electrostatic and the ion current parallel to the magnetic field is ignorable,

$$n_i \simeq (-1 + I_i) \frac{e\phi}{T_i} n_0, \tag{168}$$

where the function I_i defined by

$$I_i = \int \frac{\omega + \widehat{\omega}_{*i}}{\omega + \widehat{\omega}_{Di}} J_0^2 \left(\frac{k_\perp v_\perp}{\omega_{ci}}\right) f_{Mi} d\mathbf{v}, \tag{169}$$

involves ion kinetic resonance at $\omega + \widehat{\omega}_{Di}(\mathbf{v}) = 0$.

For the electrons, the finite Larmor radius effect may be ignored. The perturbed electron distribution function can be written down analogously,

$$f_e = \frac{e\phi}{T_e} f_{Me} - \frac{\omega - \widehat{\omega}_{*e}}{\omega - k_\parallel v_\parallel - \widehat{\omega}_{De}} \left(\phi - v_\parallel A_\parallel\right) \frac{e}{T_e} f_{Me} \tag{170}$$

where

$$\widehat{\omega}_{*e}\left(v^2\right) = \frac{T_e}{eB^2}\left[1 + \eta_e \left(\frac{mv^2}{2T_e} - \frac{3}{2}\right)\right] [\boldsymbol{\nabla}(\ln n_0) \times \mathbf{B}_0] \cdot \mathbf{k}_\perp, \tag{171}$$

$$\widehat{\omega}_{De}(\mathbf{v}) = \frac{m}{eB^3}\left(\frac{1}{2}v_\perp^2 + v_\parallel^2\right) (\boldsymbol{\nabla} B \times \mathbf{B}_0) \cdot \mathbf{k}_\perp. \tag{172}$$

In Eq. (170), effects of trapped electrons are ignored. They have relatively weak stabilizing influence on the ballooning mode through a reduction in the electron parallel current.

In the low frequency limit $|\omega| \ll k_\parallel v_{Te}$, the electron density perturbation can be approximated by

$$\begin{aligned} n_e &= \frac{e\phi}{T_e} n_0 - \left\langle \frac{\omega - \widehat{\omega}_{*e}\left(v^2\right)}{\omega + \widehat{\omega}_{De}\left(\mathbf{v}\right) - k_\parallel v_\parallel} \left(\phi - v_\parallel A_\parallel\right) \right\rangle_{\mathbf{v}} \frac{e}{T_e} n_0 \\ &\simeq \left(\phi - \frac{\omega - \omega_{*e}}{k_\parallel} A_\parallel\right) \frac{e}{T_e} n_0. \end{aligned} \tag{173}$$

The parallel current is largely carried by the electrons, and can be evaluated from the 1st order moment of the perturbed electron velocity distribution function,

$$\begin{aligned} J_{\parallel e} &= -e \int v_\parallel f_e d\mathbf{v} \\ &\simeq \frac{n_0 e^2}{k_\parallel T_e} \left[(\omega_{*e} - \omega)\phi + \frac{(\omega - \omega_{*e})(\omega - \omega_{De}) + \eta_e \omega_{*e} \omega_{De}}{k_\parallel} A_\parallel \right]. \end{aligned} \tag{174}$$

Substituting the ion and electron density perturbations into the charge neutrality condition,

$$n_e = n_i,$$

and the parallel electron current into Ampere's law,

$$\nabla_\perp^2 A_\parallel = -\mu_0 J_\parallel,$$

we obtain

$$(-1 + I_i)\frac{e\phi}{T_i} n_0 = \left(\phi - \frac{\omega - \omega_{*e}}{k_\parallel} A_\parallel\right) \frac{e}{T_e} n_0, \tag{175}$$

and

$$\nabla_\perp^2 A_\parallel = -\frac{\mu_0 n_0 e^2}{k_\parallel T_e} \left[(\omega_{*e} - \omega)\phi + \frac{(\omega - \omega_{*e})(\omega - \omega_{De}) + \eta_e \omega_{*e} \omega_{De}}{k_\parallel} A_\parallel \right]. \tag{176}$$

These two equations form a closed set for the two unknowns, ϕ and $A_\parallel$. The parallel Ampere's law can be rearranged as

$$k_\parallel k_\perp^2 k_\parallel \frac{A_\parallel}{k_\parallel} = \frac{k_{De}^2}{c^2} \left\{ (\omega_{*e} - \omega)\phi + \frac{(\omega - \omega_{*e})(\omega - \omega_{De}) + \eta_e \omega_{*e} \omega_{De}}{k_\parallel} A_\parallel \right\}. \tag{177}$$

where $k_{De}^2 = n_0 e^2 / \varepsilon_0 T_e$ is the square of the electron Debye wavenumber. Eliminating $A_\parallel$ between Eqs. (175) and (177) yields the following kinetic ballooning mode equation [21 Hirose PRL],

$$k_\parallel k_\perp^2 k_\parallel \widehat{\phi} + \frac{k_{De}^2}{c^2} \left[\frac{(\omega - \omega_{*e})^2}{1 + \tau - \tau I_i} - (\omega - \omega_{De})(\omega - \omega_{*e}) - \eta_e \omega_{*e} \omega_{De} \right] \widehat{\phi} = 0, \tag{178}$$

where $\widehat{\phi}$ is a reduced scalar potential defined by

$$\widehat{\phi} = (1 + \tau - \tau I_i)\,\phi. \tag{179}$$

After ballooning transformation, Eq. (178) is converted into a differential equation,

$$\frac{d}{d\theta}\left\{[1 + (s\theta - \alpha\sin\theta)^2]\frac{d\phi}{d\theta}\right\} + \frac{\alpha}{4\epsilon_n(1+\eta)}\left\{(\Omega-1)[\Omega - f(\theta)] + \eta f(\theta) - \frac{(\Omega-1)^2}{2 - I_i(\theta)}\right\}\phi = 0, \tag{180}$$

where $T_i = T_e$ and $\eta_e = \eta_e = \eta$ have been assumed and the mode frequency is normalized by electron diamagnetic drift frequency, $\Omega = \omega/\omega_{*e}$. In the MHD limit $|\omega| \gg \omega_*$, ω_D and $(k_\perp\rho)^2 \ll 1$, we readily recover the MHD ballooning mode equation. It is noted that the safety factor q is absorbed in the ballooning parameter

$$\alpha = q^2\frac{R}{L_n}\left[\beta_i\,(1+\eta_i) + \beta_e\,(1+\eta_e)\right],$$

and does not appear explicitly in the mode equation. This is because the ion acoustic transit effect has been ignored by assuming $\omega \gg k_\parallel c_s \simeq k_\parallel v_{Ti}\ (T_i \simeq T_e)$. When this condition becomes marginally satisfied, an integral equation approach must be employed.

Finite β effects on the toroidal η_i mode can still be analyzed by Eq. (180) as long as the ion transit frequency is negligible, $|\omega| > k_\parallel v_{Ti}$. In this limit, the ion dynamics remains electrostatic and electromagnetic effects enter mainly through electron dynamics. Eq. (180) describes both the kinetic ballooning mode and the η_i mode corrected for finite β effects. For the ballooning mode having a frequency $|\omega| \simeq k_\parallel V_A$, the condition is well satisfied relatively independent of the finite Larmor radius parameter $k_\perp\rho$. However, for the toroidal η_i mode, the eigenvalue ω scales with $\omega_* \propto k_\perp\rho$ and the condition $|\omega| > k_\parallel v_{Ti}$ is satisfied only for comparatively short cross-field wavelengths.

In contrast to the η_i mode, the trapped electron drift ballooning mode is further destabilized by β. Eq. (180) is, unfortunately, inapplicable to analyzing the mode because in the long wavelength regime, the mode frequency approaches the ion acoustic transit frequency $k_\parallel c_s \simeq k_\parallel v_{Ti}$ $(T_e \simeq T_i)$ and the assumption $\omega \gg k_\parallel v_{Ti}$ breaks down. A rigorous analysis on finite β effects on the ion acoustic mode requires integral equation formulation.

Figure 9 shows stabilizing effect of total α (ballooning parameter) on the toroidal η_i mode in various conditions [22 Hirose PoP]. In (a), $L_n/R = 0.2$, $\eta_i = \eta_e = 2$, in (b), $L_n/R = 0.5$ (nearly flat density profile), $\eta_i = \eta_e = 4$, and in (c), same condition as in (a) except trapped electrons are included ($r/R = 0.2$). Common parameters are: $(k_\theta\rho)^2 = 0.1$, $s = 1$, $T_i = T_e$. Stabilization of the toroidal η_i mode occurs when the ballooning parameter α exceeds a threshold which depends on discharge parameters. Trapped electrons have a destabilizing effect on the η_i mode. (This is in contrast to the case of the kinetic ballooning mode which tends to be stabilized by trapped electrons.) The critical α_e required for stabilization of the η_i mode is approximately given by

$$\alpha_e \gtrsim \frac{1+\eta_e}{3\left(1-\sqrt{\varepsilon}\right)} \frac{\tau^2}{\left(1+2\varepsilon_n\right)(\tau+1)+\tau^2\eta_e}, \tag{181}$$

where $\varepsilon = r/R$, $\tau = T_e/T_i$, $\varepsilon_n = L_n/R$.

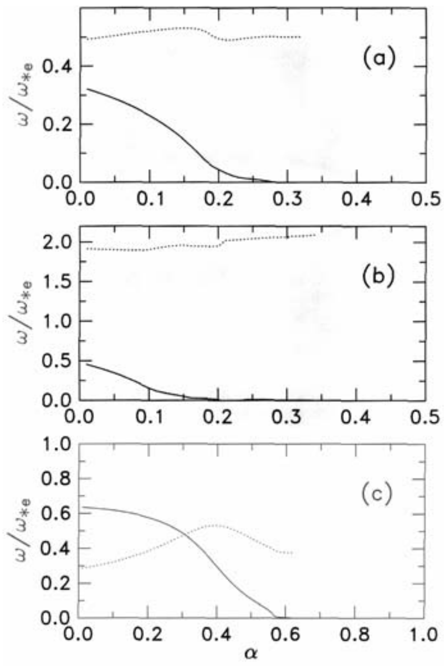

Fig. 9. Stabilization of the η_i mode by α, the ballooning parameter. Solid lines show growth rate γ/ω_{*e} and dashed lines mode frequency ω_r/ω_{*e}. $s = 1$, $\tau = T_e/T_i = 1$, $b_0 = (k_\theta \rho)^2 = 0.1$. (a) $L_n/R = 0.2$, $\eta_i = \eta_e = 2$, $r/R = 0$ (no trapped electrons). (b) $L_n/R = 0.5$, $\eta_i = \eta_e = 4$, $r/R = 0$. (c) Same as (a) except $r/R = 0.2$.

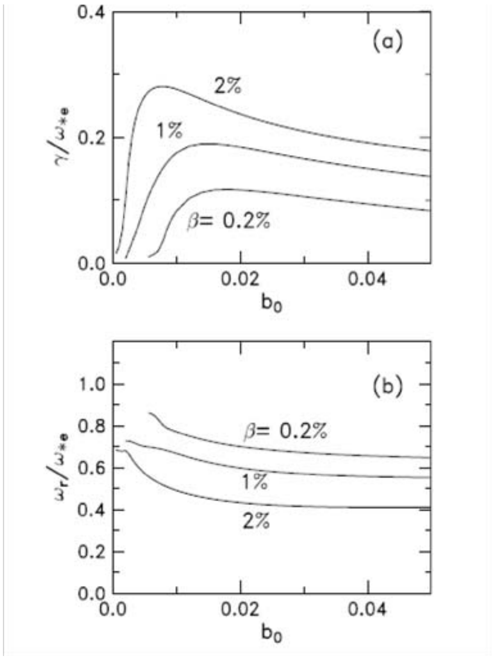

Fig. 10. β destabilization of the trapped electron drift ballooning mode. $s = 1$, $\tau = 1$, $q = 2$, $\varepsilon = 0.2$, $\varepsilon_n = 0.4$, $\eta_i = \eta_e = 1$.

Figure 10 shows finite β destabilization of the long wavelength drift mode driven by trapped electrons as found from integral equation analysis [23 Hirose-Elia CJP].

10 Kinetic Ballooning Mode

With the numerical techniques described in the preceding section, we now present the results of stability analysis of the kinetic ballooning mode. Before presenting results of kinetic analysis of the ballooning mode, let us briefly review the ideal MHD ballooning analysis. In ideal MHD, the electric field parallel to the magnetic field is assumed to be zero. (Otherwise, an infinitely large current would flow.) Then,

$$\mathbf{E}_\parallel = -\nabla_\parallel \phi - \frac{\partial \mathbf{A}_\parallel}{\partial t} = 0, \;\; k_\parallel \phi = \omega A_\parallel. \tag{182}$$

The parallel Ampere's law $\nabla_\perp^2 A_\parallel = -\mu_0 J_\parallel$ and charge neutrality $\nabla \cdot \mathbf{J} = 0$ yield

$$\nabla \cdot \nabla_\perp^2 \mathbf{A}_\parallel = -\mu_0 \nabla \cdot \mathbf{J}_\parallel = \mu_0 \nabla \cdot \mathbf{J}_\perp, \tag{183}$$

where the cross-field current consists of the the difference between the ion and electron $E\times B$ drifts, the ion polarization current and perturbed diamagnetic current,

$$\begin{aligned}\nabla\cdot\mathbf{J}_{\perp} &= -\nabla\cdot\left(n_0 e\left(k_\perp\rho_i\right)^2\frac{\mathbf{B}\times\nabla\phi}{B^2}\right)+\nabla\cdot\left(\frac{n_0 e^2}{m_i\omega_{ci}^2}\left(\frac{\partial}{\partial t}+\mathbf{V}_{Di}\cdot\nabla\right)\left(-\nabla_\perp\phi\right)\right)+\nabla\cdot\left(\frac{\mathbf{B}\times\nabla\tilde{p}}{B^2}\right)\\ &= -i\varepsilon_0\left[\omega+\left(1+\eta_i\right)\omega_{*i}\right]\frac{\omega_{pi}^2}{\omega_{ci}^2}k_\perp^2\phi-2\frac{\nabla B}{B^3}\cdot\left(\mathbf{B}\times\nabla\tilde{p}\right),\end{aligned} \tag{184}$$

where the following cancellation is noted:

$$n_0 e\frac{2}{B^3}\left(k_\perp\rho_i\right)^2\nabla B\cdot\mathbf{B}\times\nabla\phi+\frac{n_0 e^2}{m_i\omega_{ci}^2}k_\perp^2\mathbf{V}_{Di}\cdot\nabla\phi=0.$$

The perturbed plasma pressure may be approximated by

$$\frac{\partial\tilde{p}}{\partial t}+\frac{\mathbf{B}\times\nabla\phi}{B^2}\cdot\nabla p_0=0. \tag{185}$$

Then Eq. (183) reduces to

$$V_A^2 k_\parallel k_\perp^2 k_\parallel\phi=k_\perp^2\omega^2+\frac{\omega_{*p}\omega_{De}}{\rho_s^2}, \tag{186}$$

where $|\omega|\gg\omega_{*i}$ is assumed and

$$\omega_{*p}=\left(1+\eta_e\right)\omega_{*e}+\left(1+\eta_i\right)\omega_{*i}, \tag{187}$$

$$\omega_{De}=\frac{2T_e}{eBR}\mathbf{k}\cdot\mathbf{e}_z. \tag{188}$$

Noting $k_\parallel=-i\frac{1}{qR}\partial/\partial\theta$, Eq. (186) can be converted to the following ballooning equation [24 Connor, Hastie, Taylor]

$$\begin{aligned}&\frac{d}{d\theta}\left\{\left[1+\left(s\theta-\alpha\sin\theta\right)^2\right]\frac{d\phi}{d\theta}\right\}+\alpha\left[\cos\theta+\left(s\theta-\alpha\sin\theta\right)\right]\phi\\ &\qquad+\left(\omega/\omega_A\right)^2\left[1+\left(s\theta-\alpha\sin\theta\right)^2\right]\phi=0,\end{aligned} \tag{189a}$$

where $\omega_A=V_A/qR$ is the Alfven frequency and ω_{*i} has been ignored. This equation has been studied extensively in the past. Stable-unstable boundaries in the (s,α) plane are shown in Fig. 11. For a given shear s, a tokamak discharge becomes ballooning unstable above a critical α. A further increase in α stabilizes the ideal MHD ballooning mode [25 Mercier, 26 Sykes, 27 Zakharov].

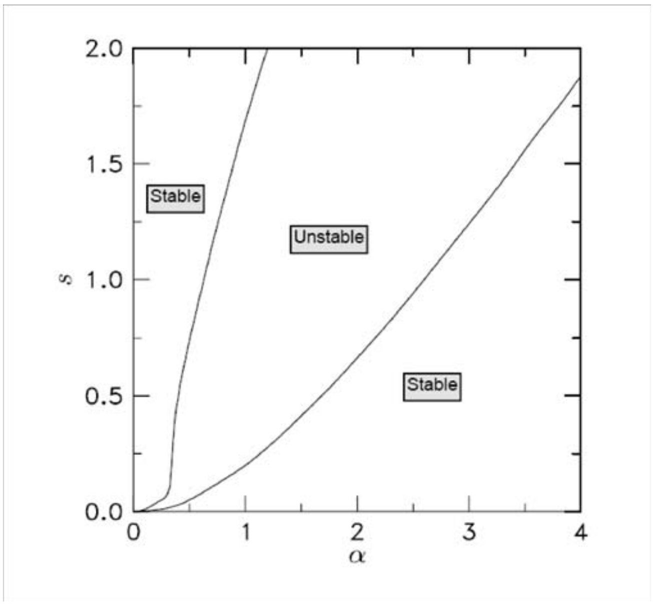

Fig. 11. Tokamak stability boundary for the ideal MHD ballooning mode in the (s, α) plane.

More rigorous analysis based on the kinetic mode equation, Eq. (180), essentially nullifies the so-called second stability regime when the ion temperature gradient (η_i) is finite [21]. In Fig. 12 (a) and (b), the growth rate and mode frequency normalized by the Alfven frequency , γ/ω_A and ω_r/ω_A ($\omega_A = V_A/qR$) are shown when $s = 0.4$, $b_0 = (k_\theta \rho)^2 = 0.01$, $\eta_i = \eta_e = 2$, $\epsilon_n = L_n/R = 0.175$. As far as the maximum growth rate is concerned, the MHD and kinetic theories agree well. The critical α for the onset of the ballooning mode from the kinetic theory is $\alpha_c = 0.35$, which is somewhat smaller than that obtained from the ideal MHD theory, $\alpha_c = 0.39$. The dashed line shows a second mode revealed by the kinetic analysis.

The growth rate revealed from the kinetic analysis persists in the MHD second stability region. The kinetic ballooning mode in the MHD second stability regime requires a finite ion temperature gradient, $\eta_i \gtrsim 1$, and is driven through the resonance contained in the non-adiabatic ion density perturbation, $I_i(\theta)$.

At small shear, the critical α for the (kinetic) ballooning mode becomes small and the instability becomes threshold-less and remains unstable at any α. Fig. 13 shows the case $s = 0.2$ with other parameters unchanged from those in Fig. 12.

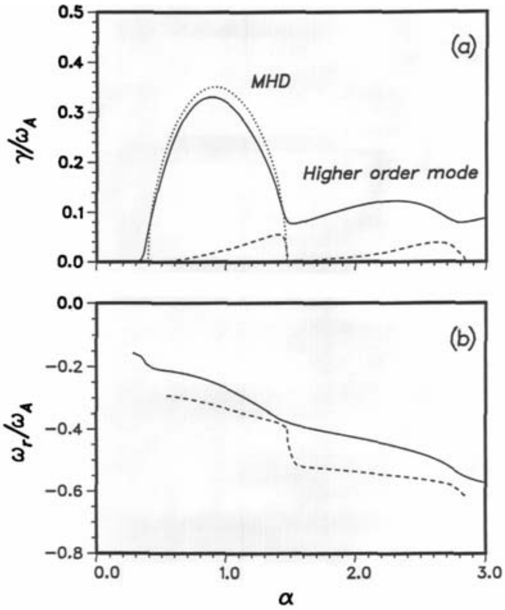

Fig. 12. Growth rate γ/ω_A and frequency ω_r/ω_A of the kinetic ballooning mode vs. α when $s = 0.4$, $q = 2$, $b_0 = 0.01$, $T_i = T_e$, $L_n/R = 0.175$, $\eta_i = \eta_e = 2$. The dotted line shows the growth rate of the ideal MHD ballooning mode and dashes lines show the second kinetc ballooning mode.

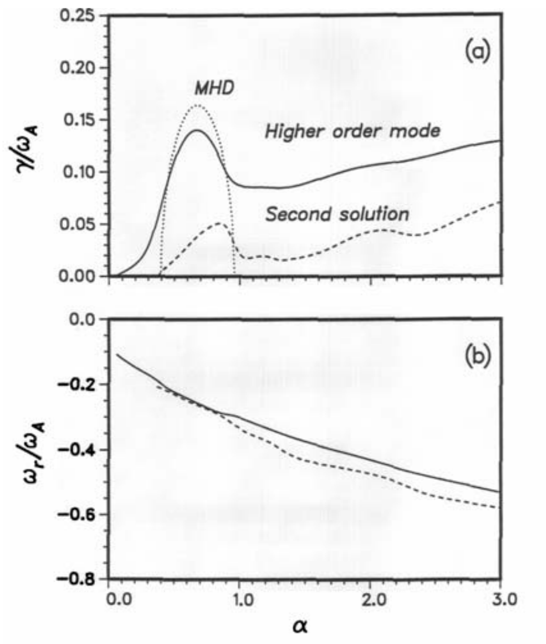

Fig. 13. Same as Fig. 12 except $s = 0.2$.

11 Short Wavelength Drift Modes

Often the short wavelength electron temperature gradient (ETG) mode is considered to be the dual of the long wavelength ITG mode. In the ITG mode, the electron response is adiabatic (except for the destabilizing trapped electron contribution), while in the ETG mode, the ion response is adiabatic, since the nonadiabatic term proportional to $e^{-b_i}I_0(b_i)$ vanishes in the short wavelength regime of electron Larmor radius, $b_i = (k_\perp \rho_i)^2 \simeq m_i/m_e \gg 1$. (An exception is the case when $\omega_{Di} < |\omega| < \omega_{*i}$. In this intermediate frequency regime, the ion density perturbation becomes nearly independent of $k_\perp \rho_i$,

$$\begin{aligned} n_i &= -\frac{e\phi}{T_i}n_0 + \frac{\omega+\omega_{*i}}{\omega+\omega_{Di}}e^{-b_i}I_0(b_i)\frac{e\phi}{T_i}n_0 \\ &\simeq -\frac{e\phi}{T_i}n_0 + \frac{\omega_{*i}}{\omega}\frac{1}{\sqrt{2\pi b_i}}\frac{e\phi}{T_i}n_0, \ \ b_i \gg 1 \end{aligned} \tag{190}$$

since $\omega_{*i} \propto \sqrt{b_i}$. An ITG mode in such short wavelength regime has recently been identified [28 Smolyakov]. It is a slab-like mode and toroidicity has a stabilizing influence.) However, tokamaks are normally operated in a strong magnetic field such that $\omega_{ce} > \omega_{pe}$, or $\rho_e < \lambda_{De}$ where λ_{De} is the electron Debye length. Therefore, charge neutrality may not hold and duality could breaks down. In this case, normalization of the cross field wavelength by the electron Debye length is more convenient.

Analysis of ETG mode in tokamaks without imposing charge neutrality has revealed that the maximum growth rate occurs at $d_e = k_\theta/k_{De} \simeq 0.7$. The mode is predominantly electrostatic. Charge nonneutrality introduces a normalized electron temperature T_e/mc^2 as another dimensionless parameter in tokamak stability analysis. The growth rate is proportional to $\sqrt{\beta_e}$ even though the mode is electrostatic. The mixing length electron thermal diffusivity is approximately given by [29 Hirose PRL 04]

$$\chi_e \simeq q\frac{v_{Te}}{L_{Te}}\left(\frac{c}{\omega_{pe}}\right)^2\sqrt{\beta_e}, \tag{191}$$

where L_{Te} is the scale length of electron temperature gradient and c/ω_{pe} is the electron skin depth.

To analyze drift modes in the regime $b_i > 1$, we continue to employ the gyro-kinetic equations subject to the conditions that $\omega \ll \omega_{ci}$ ($\ll \omega_{ce}$). The maximum frequency and growth rate of interest does not exceed the electron transit frequency $\omega_{Te} = \sqrt{T_e/m_e}/qR$. The condition $\omega \simeq \omega_{Te}$ $\ll \omega_{ci}$ becomes

$$\rho_e \ll \frac{m_e}{m_i}qR,$$

where ρ_e is the electron Larmor radius which is of the order of 10^{-4} m or less, while the RHS $\frac{m_e}{m_i} qR \simeq 10^{-3}$ m. Therefore, the condition $\omega \ll \omega_{ci}$ is satisfied with a large margin. The second condition $\rho_i \ll L_{Te}$ is also well satisfied even in the internal transport barrier (ITB) characterized by steep density and temperature gradient. In the ETG mode, ions are essentially adiabatic,

$$n_i \simeq -\frac{e\phi}{T_i} n_0,$$

particularly in the regime where the growth rate peaks. As will be shown, this occurs at $k_\perp \simeq 0.7 k_{De}$ where k_{De} is the electron Debye wavenumber. However, in the lower end of the k spectrum (long wavelength cutoff), the wavelength approaches the electron skin depth, $k_\perp \simeq \omega_{pe}/c$, where ions are not adiabatic. Note that c/ω_{pe} is comparable with the ion Larmor radius ρ_i. The ratio is

$$\frac{\omega_{pe}\rho_i}{c} = \sqrt{\frac{m_i}{m_e}\frac{4\pi n T_i}{B^2}} = \sqrt{\frac{m_i}{2m_e}\beta_i}, \tag{192}$$

where

$$\beta_i = \frac{2\mu_0 n T_i}{B^2},$$

is the ion beta factor. The quantity $\sqrt{\frac{m_i}{2m_e}\beta_i}$ falls in the range 1 to 4 in high performance tokamaks. In order to cover the entire spectrum of the ITG and ETG modes satisfactorily, fully kinetic ion and electron responses without the assumption of adiabatic ions or electrons must be employed by appropriately implementing the electron transit effect, $k_\parallel v_{Te}$. This requires formulation in terms of integral equations.

The basic field equations are the Poisson's equation,

$$\nabla^2\phi = -\frac{1}{\varepsilon_0} e \left[n_i(\phi, A_\parallel) - n_e(\phi, A_\parallel) \right], \tag{193}$$

and the parallel Ampere's law,

$$\nabla_\perp^2 A_\parallel = -\mu_0 J_\parallel(\phi, A_\parallel), \tag{194}$$

where the density perturbations are given in terms of the perturbed velocity distribution functions f_i and f_e as

$$n_i = \int f_i d\mathbf{v}, \quad n_e = \int f_e d\mathbf{v}, \tag{195}$$

and the parallel current by

$$J_\parallel = e\int v_\parallel (f_i - f_e) d\mathbf{v}. \tag{196}$$

The distribution functions f_i and f_e are given by

$$f_i = -\frac{e\phi}{T_i} f_{Mi} + g_i(v,\theta) J_0(\Lambda_i), \tag{197}$$

$$f_e = \frac{e\phi}{T_e} f_{Me} + g_e(v,\theta) J_0(\Lambda_e), \tag{198}$$

where $g_{i,e}$ are the nonadiabatic parts that satisfy

$$\left(i\frac{v_\parallel(\theta)}{qR}\frac{\partial}{\partial\theta} + \omega + \widehat{\omega}_{Di} \right) g_i = (\omega + \widehat{\omega}_{*i}) J_0(\Lambda_i) \left(\phi - v_\parallel A_\parallel\right) \frac{e}{T_i} f_{Mi}, \tag{199}$$

$$\left(i\frac{v_\parallel(\theta)}{qR}\frac{\partial}{\partial\theta} + \omega - \widehat{\omega}_{De} \right) g_e = -(\omega - \widehat{\omega}_{*e}) J_0(\Lambda_e) \left(\phi - v_\parallel A_\parallel\right) \frac{e}{T_e} f_{Me}. \tag{200}$$

Here, θ is the extended poloidal angle, ϕ is the scalar potential, $A_\parallel$ is the parallel vector potential, J_0 is the Bessel function with argument $\Lambda_{i,e} = k_\perp v_\perp/\omega_{ci,e}$, and qR is the connection length.

For circulating particles, g_j $(j = i, e)$ can be integrated as [30 Rewoldt]

$$v_\parallel > 0, \qquad g_j^+ = -i\frac{e_j f_{Mj}}{T_j}\int_{-\infty}^{\theta} d\theta' \frac{qR}{|v_\parallel|} e^{i\beta_j} (\omega - \widehat{\omega}_{*j}) J_0(\Lambda_j') \left(\phi(\theta') - \left|v_\parallel\right| A_\parallel(\theta')\right), \tag{201}$$

$$v_\parallel < 0, \qquad g_j^- = -i\frac{e_j f_{Mj}}{T_j}\int_{\theta}^{\infty} d\theta' \frac{qR}{|v_\parallel|} e^{-i\beta_j} (\omega - \widehat{\omega}_{*j}) J_0(\Lambda_j') \left(\phi(\theta') + \left|v_\parallel\right| A_\parallel(\theta')\right), \tag{202}$$

where

$$\beta_j(\theta,\theta') = \int_{\theta'}^{\theta} \frac{qR}{|v_\parallel|} [\omega - \widehat{\omega}_{Dj}(\theta'')] d\theta''.$$

For trapped particles with turning points θ_1 and θ_2 $(\theta_2 > \theta_1)$, the solution is

$$g^\sigma = \frac{e^{i\sigma\beta_j(\theta,\theta')\sin(\theta-\theta')}}{2\sin[\beta(\theta,\theta')]} \int_{\theta_1}^{\theta_2} \left(e^{-i\beta(\theta_2,\theta')\mathrm{sgn}(\theta)} + e^{i\beta(\theta_2,\theta')\mathrm{sgn}(\theta)} \right) d\theta' - i\sigma \int_{\theta_1}^{\theta} e^{i\sigma\beta(\theta,\theta')} \gamma_\sigma d\theta', \tag{203}$$

where $\sigma = \mathrm{sgn}(v_\parallel)$,

$$\gamma_\sigma = \gamma_\phi + \sigma\gamma_A, \tag{204}$$

$$\gamma_\phi = \frac{e_j}{T_j}\frac{qR}{|v_\parallel|}(\omega - \omega_{*j}) J_0(\Lambda_j) \phi(\theta') f_{Mj}, \tag{205}$$

$$\gamma_A = -\frac{e_j}{T_j}\frac{qR}{|v_\parallel|}(\omega - \omega_{*j})J_0(\Lambda_j)\left|v_\parallel\right| A_\parallel(\theta')f_{Mj}. \tag{206}$$

Since for electrons, $\beta(\theta_2, \beta_1)$ is of order of $\omega/\omega_{be} \ll 1$ where ω_{be} is the electron bounce frequency, trapped electron response may be approximated by

$$g_e^\sigma \simeq \frac{1}{2\beta(\theta_2,\theta_1)}\int_{\theta_1}^{\theta_2}(\gamma_\phi + i\beta(\theta_2,\theta')\gamma_A)d\theta' - i\int_{\theta_1}^{\theta}\gamma_A d\theta'. \tag{207}$$

In this analysis, we ignore trapped ions since the frequency regime of interest is at least of the order of the ion transit frequency. Substitution of perturbed distribution functions into charge neutrality and parallel Ampere's law yields

$$\nabla^2\phi = -\frac{1}{\varepsilon_0}\sum_j e_j\left(-\frac{e_j}{T_j}\phi + \int\left[g_j^+(\theta) + g_j^-(\theta)\right]J_0(\Lambda_j)d\mathbf{v}\right), \tag{208}$$

$$\nabla_\perp^2 A_\parallel(\theta) = -\mu_0\sum_j e_j\int v_\parallel\left[g_j^+(\theta) - g_j^-(\theta)\right]J_0(\Lambda_j)d\mathbf{v}, \tag{209}$$

where $\int d\mathbf{v} = 2\pi\int_0^\infty v_\perp dv_\perp \int_0^\infty dv_\parallel$. This system of inhomogeneous integral equations can be solved by employing the method of Fredholm in which the integral equations are viewed as a system of linear algebraic equations.

12 The ETG Mode

In this Section, we investigate stability of drift modes in the regime $\omega_{pe}/c \lesssim k_\perp \lesssim 1/\rho_e$ where c/ω_{pe} is the electron skin depth and ρ_e is the electron Larmor radius. Ions tend to be adiabatic in such regime and we are primarily concerned with the ETG mode. In tokamaks, $\rho_e < \lambda_{De}$ (or $\omega_{ce} > \omega_{pe}$) generally holds. Therefore it is not appropriate to assume charge neutrality in studying the ETG mode. If charge neutrality does not hold, that is, if the term $(k/k_{De})^2$ is not negligible, there arises apparent dependence of ω on plasma β even in the electrostatic limit. With adiabatic ions, the electrostatic dispersion relation of the ETG mode is

$$1 + \tau + \left(\frac{k}{k_{De}}\right)^2 = \left\langle \frac{\omega - \widehat{\omega}_{*e}}{\omega - \widehat{\omega}_{De} - k_\parallel v_\parallel}J_0^2(\Lambda_e)\right\rangle. \tag{210}$$

The charge nonneutrality factor $(k/k_{De})^2 \simeq (k_\perp/k_{De})^2$ and the electron finite Larmor radius parameter $(k_\perp\rho_e)^2$ are related through

$$\left(\frac{k_\perp}{k_{De}}\right)^2 = (k_\perp\rho_e)^2\frac{2}{\beta_e}\frac{T_e}{mc^2}, \tag{211}$$

where T_e/mc^2 is the normalized electron temperature. Even in the electrostatic mode equation (and resultant dispersion relation), β_e has to be specified because the ballooning parameter $\alpha_e = q^2 R\beta_e/L_{pe}$ is one of the parameters to characterize plasma equilibrium. The electron FLR parameter $k_\perp \rho_e$ is of course the key parameter in gyro-kinetic formulation. Therefore, when charge neutrality does not hold, the normalized temperature T_e/mc^2 has to be specified together with various other dimensionless parameters. For a given electron temperature, charge nonneutrality is evidently more enhanced at lower plasma density. Since the term $(k/k_{De})^2$ is stabilizing, it is expected that the growth rate of the ETG mode becomes dependent on β_e. The growth rate of the ETG mode with charge neutrality $(k_\perp/k_{De})^2 \ll 1$ and negligible electron transit frequency $\omega \gg k_\parallel v_{Te}$ is approximately given by

$$\gamma \simeq \sqrt{\eta_e \omega_{*e} \omega_{De}/\tau}. \tag{212}$$

Charge non-neutrality reduces the growth rate as

$$\gamma \simeq \sqrt{\frac{\eta_e \omega_{*e} \omega_{De}}{\tau + (k_\perp/k_{De})^2}}. \tag{213}$$

In short wavelength regime $(k_\perp/k_{De})^2 > \tau$, the growth rate approaches

$$\gamma \simeq c\sqrt{\frac{\beta_e}{L_T R}}, \tag{214}$$

being proportional to $\sqrt{\beta_e}$.

To demonstrate the importance of charge nonneutrality in the ETG mode, we show in Fig. 14 the dependence of mode frequency and growth rate, both normalized by the electron transit frequency $\omega_{Te} = v_{Te}/qR$, on the normalized perpendicular wavenumber, $d_e = (k_\theta/k_{De})^2$, for three values of β, $\beta_e = \beta_i = 0.1\%$, 0.2% and 0.5% when $T_e = T_i = 10$ keV $\left(T_e/m_e c^2 \simeq 0.02\right)$. Other parameters assumed are: $L_n/R = 0.2$, $s = 1$, $q = 2$, $\eta_e = \eta_i = 2$, $m_i/m_e = 1836$ (hydrogen). The maximum growth rate occurs approximately at a constant value of $(k_\theta/k_{De})^2 \simeq 0.5$ when the plasma density and electron temperature are varied. If the conventional normalization $b_e = (k_\theta \rho_e)^2$ is used, the maximum growth rate occurs at widely different values of b_e. When charge neutrality does not hold, normalization in the form $(k_\theta/k_{De})^2$ is thus more appropriate.

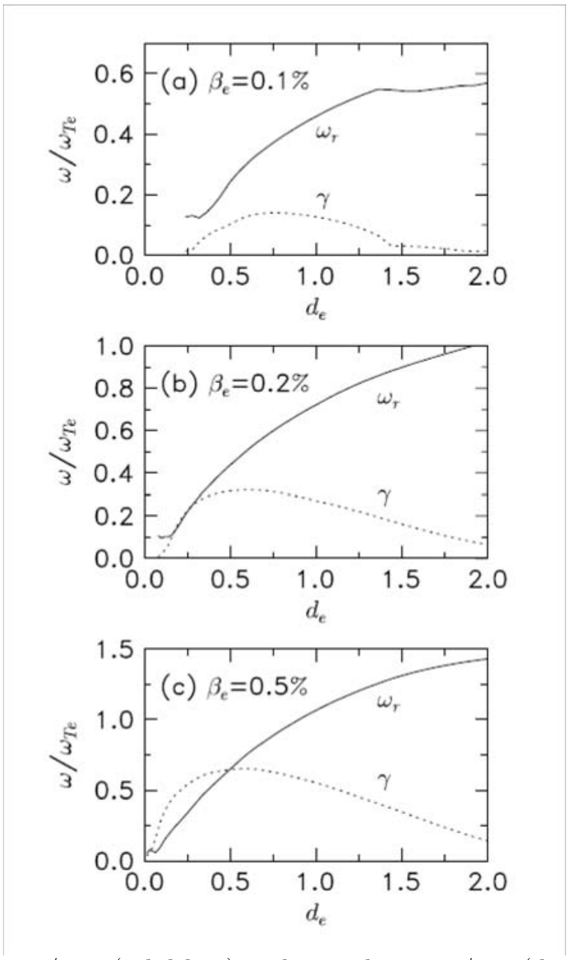

Fig. 14. Mode frequency ω_r/ω_{Te} (solid line) and growth rate γ/ω_{Te} (dotted line) as functions of $d_e = (k_\theta/k_{De})^2$ when $T_e = T_i = 10$ keV, $s = 1$, $\tau = 1$, $\varepsilon_n = 0.2$, $\eta_i = \eta_e = 2$, $q = 2$, $m_i/m_e = 1836$. β_e $(= \beta_i)$ is scanned from 0.1 to 0.5%.

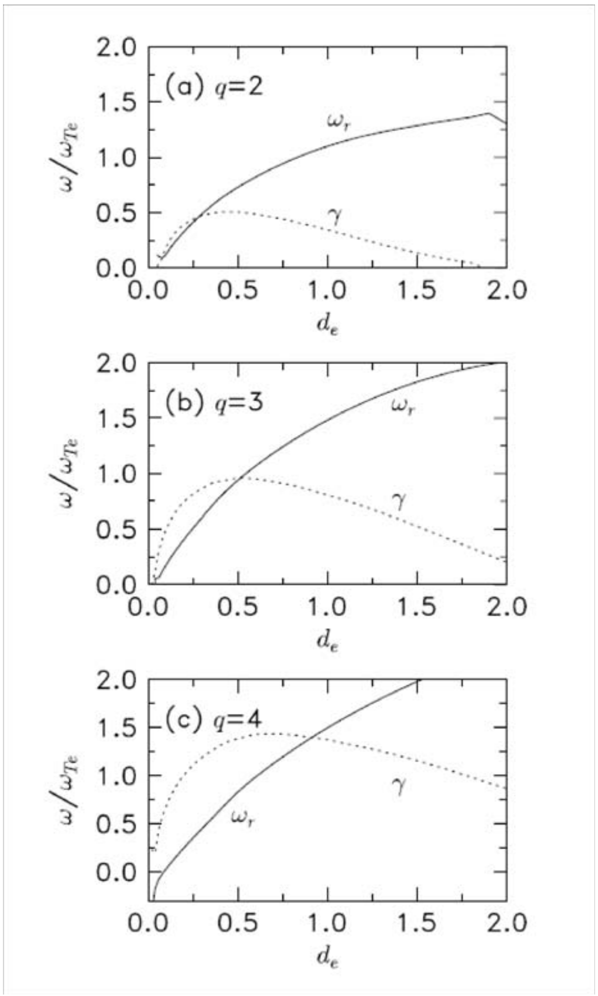

Fig. 15. q dependence of $(\omega_r + i\gamma)/\omega_{Te}$ when $T_e = T_i = 5$ keV, $\beta_e = \beta_i = 0.2\%$, $s = 1$, $\tau = 1$, $\varepsilon_n = 0.2$, $\eta_i = \eta_e = 2$, $m_i/m_e = 1836$.

It is noted that mode frequency ω is of the order of the electron transit frequency, $\omega_{Te} = v_{Ti}/qR$. This is the major difference from the long wavelength ITG mode in which the ion transit frequency is subdominant, $|\omega| > v_{Ti}/qR$. Electron parallel Landau damping thus plays a major role in the ETG mode. Since $k_{\parallel} \simeq 1/qR$, the mode frequency is expected to be sensitively dependent on the safety factor q. This is shown in Fig. 15 for $T_e = 10$ keV. A relatively small value of $\beta_e = 0.2\%$ is chosen to keep the ballooning parameter α, which is proportional to q^2, below the limit of drift reversal. The maximum growth rate γ/ω_{Te} increases with q in a manner approximately proportional to q^2, $\gamma_{\max}/\omega_{Te} \propto q^2$. Since $\omega_{Te} = v_{Te}/qR$, the unfolded growth rate is proportional to q.

13 Mixing Length Estimate of χ_i and χ_e

In this Section, mixing length estimates of the electron thermal diffusivity,

$$\chi_{i,e} = \frac{\gamma^3}{\omega_r^2 + \gamma^2} \frac{1}{k_\perp^2}, \tag{215}$$

are presented for the ITG and ETG modes. Fig. 16 shows how the ITG driven ion thermal diffusivity χ_i depends on the safety factor q. χ_i is normalized by $c_s \rho_s^2 / L_n$. In the scan in (a), the ballooning parameter remains below the threshold of finite α stabilization. It can be seen that χ_i increases with q almost linearly. In the case shown in (b), β is large and the ballooning parameter exceeds the threshold for stabilization of the ITG mode at $q \simeq 3.5$. The sudden reduction in χ_i at $q = 4$ is due to deactivation of the ITG mode. The analysis of the ITG mode has yielded the following ion thermal diffusivity,

$$\chi_i \simeq 0.1 q \sqrt{\frac{R}{L_{Ti}}} \frac{v_{Ti} \rho^2}{L_{Ti}}.$$

The relationship $\chi_i \propto q$ arises from the coupling to the ion acoustic transit mode in the long wavelength regime.

Figure 17 shows ETG driven electron thermal diffusivity χ_e in units of $(v_{Te}/qR)/k_{De}^2$ when $\beta_e = 0.2\%$, $T_e = T_i = 5$ keV and 10 keV. The safety factor q is scanned between $q = 2$ and 4. The maximum value of χ_e is proportional to q^2 but inversely proportional to the temperature. Since $\omega_{Te} \propto 1/q$, this suggests that the electron thermal diffusivity is also proportional to q and has the following scaling,

$$\chi_e \propto \frac{q v_{Te}}{n_0}.$$

Results of scanning β_e, electron temperature T_e, and the safety factor q can be summarized by the following electron thermal diffusivity,

$$\chi_e \simeq \frac{q v_{Te}}{L_T} \left(\frac{c}{\omega_{pe}} \right)^2 \sqrt{\beta_e}. \tag{216}$$

Earlier, Ohkawa proposed the following diffusivity [31],

$$\chi_e = \frac{v_{Te}}{qR} \left(\frac{c}{\omega_{pe}} \right)^2, \tag{217}$$

assuming that the electron skin depth plays the role of cross-field random walk distance and taking the electron transit frequency v_{Te}/qR as the inverse correlation time. The diffusivity revealed in the present study is proportional to q which is attributed to the coupling to the electron transit frequency. It has recently been reported that both ion and electron thermal diffusivities in the DIII-D tokamak are approximately proportional to the safety factor [32].

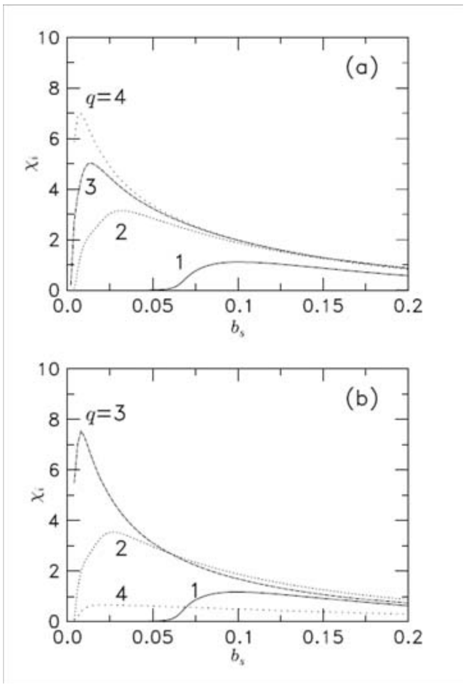

Fig. 16. Ion thermal diffusivity due to the ITG mode normalized by $c_s\rho_s^2/L_n$ vs. $b_s = (k_\theta \rho_s)^2$ when q is varied. (a) $\beta_i = \beta_e = 10^{-4}$, (b) $\beta_i = \beta_e = 10^{-3}$. Common parameters are: $\varepsilon_n = 0.2$, $\varepsilon = 0.1$, $\eta_i = \eta_e = 2$, $s = 1$, $T_i = T_e$, $m_i/m_e = 1836$.

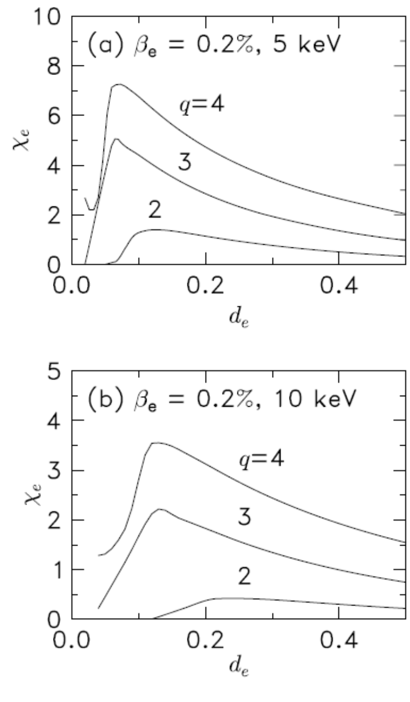

Fig. 17. χ_e in units of ω_{Te}/k_{De}^2 vs. $d_e = (k_\theta/k_{De})^2$ when $\beta_e = \beta_i = 0.2\%$ and $q = 2, 3, 4$. In (a), $T_e = T_i = 5$ keV and in (b), $T_e = T_i = 10$ keV.

Acknowledgements

The author has benefitted from discussions with Mike Elia, Jan Weiland, Atsushi Ito, and Swadesh Mahajan.

This research has been supported by the Natural Sciences and Engineering Research Council of Canada and by Canada Research Chair Program.

References

1. For a comprehensive review of the earlier work, see, for example, B. B. Kadomtsev, *Plasma Turbulence*, (Academic Press, New York, 1965); A. B. Mikahilovskii, *Reviews of Plasma Physics*, Vol. 3, (Consultants Bureau, New York, 1967), p. 159.
2. N. A. Krall and M. N. Rosenbluth, Phys. Fluids **8**, 1488 (1965).
3. L. D. Pearlstein and H. L. Berk, Phys. Rev. Lett. **23**, 220 (1969).
4. D. W. Ross and S. Mahajan, Phys. Rev. Lett. **40**, 324 (1978).
5. K. T. Tsang, P. J. Catto, J. C. Whitson, and J. Smith, Phys. Rev. Lett. **40**, 327 (1978).
6. C. Z. Cheng and L. Chen, Phys. Fluids **23**, 1770 (1980).
7. K. W. Hesketh, Nucl. Fusion **20**, 1013 (1980).
8. A. Jarmen, P. Andersson, and J. Weiland, Nucl. Fusion **27**, 941 (1987).
9. Y. C. Lee, J. Q. Dong, P. N. Guzdar, and C. S. Liu, Phys. Fluids **30**, 1331 (1987).
10. J. Weiland and A. Hirose, Nucl. Fusion **32**, 151 (1992).
11. L. Tonks, Phys. Rev. **97**, 1443 (1955).
12. B. D. Fried and S. D. Conte, *The Plasma Dispersion Function*, (Academic Press, New York, 1961).
13. M. Sato, *Lecture Notes on Plasma Stability*, (Summer School on Plasma Physics, Gifu, 1966).
14. L. I. Rudakov and R. Z. Sagdeev, Dokl. Akad. Nauk SSR **138**, 581 (1961).
15. B. Coppi, A. Ferreira, J.W.-K. Mark, and J.J. Ramos, Nucl. Fusion **19**, 715 (1979).
16. A. Hirose, Phys. Fluids B **3**, 1599 (1991).
17. M. Elia, Ph.D. dissertation, University of Saskatchewan (2000).
18. H. Hojo and T. Watanabe, J. Phys. Soc. Japan **45**, 2053 (1978).
19. A. Hirose, M. Elia, A. I. Smolyakov, and M. Yagi, Phys. Plasmas **9**, 1659 (2002).

20. A. Hirose and M. Elia, Phys. Plasmas **9**, 4664 (2002).

21. A. Hirose, L. Zhang, and M. Elia, Phys. Rev. Lett **72**, 3993 (1994).

22. A. Hirose, Phys. Plasmas **7**, 433-436 (2000).

23. A. Hirose and M. Elia, Can. J. Phys. **78**, 277 (2000).

24. J. W. Connor, R. J. Hastie, and J. B. Taylor, Phys. Rev. Lett. **40**, 396 (1978).

25. C. Mercier, Plasma Physics and Controlled Nuclear Fusion Research, (IAEA, Vienna, 1978), Vol. 1, p. 701,

26. A. Sykes and M.F. Turner, *ibid.*, p. 625.

27. L. E. Zakharov, *ibid.*, p. 689.

28. A. Smolyakov, M. Yagi, and K. Kishimoto, Phys. Rev. Lett. 125005 (2002).

29. A. Hirose, Phys. Rev. Lett. **92**, 025001 (2004).

30. G. Rewoldt, W. M. Tang, and R. J. Hastie, Phys. Fluids **30**, 807 (1987).

31. T. Ohkawa, Phys. Lett. A **67**, 35 (1978).

32. C. C. Petty, J. E. Kinsey, and T. C. Luce, Phys. Plasmas **11**, 1011 (2004).